

UCSF

UC San Francisco Electronic Theses and Dissertations

Title

Investigating non-canonical mechanisms of receptor tyrosine kinase signaling

Permalink

<https://escholarship.org/uc/item/68s4s5g6>

Author

Frazier, Nicole Michael

Publication Date

2018

Peer reviewed|Thesis/dissertation

Investigating non-canonical mechanisms of receptor tyrosine kinase
signaling

by

Nicole Amber Michael Frazier

DISSERTATION

Submitted in partial satisfaction of the requirements for the degree of

DOCTOR OF PHILOSOPHY

in

Biochemistry and Molecular Biology

in the

GRADUATE DIVISION

of the

UNIVERSITY OF CALIFORNIA, SAN FRANCISCO

Acknowledgements

Getting a PhD is a monumental endeavor that requires hard work, patience, grit, and above all support from mentors, friends, and loved ones. I would not have accomplished this without the help and support of many wonderful people.

First, I would like to thank my advisor Natalia Jura. When I started working with Natalia, the lab was still in its infancy. I was most drawn to Natalia's hard work ethic, creative thinking, and especially her absolute passion and enthusiasm for science. Her help has been invaluable and we have both grown as mentor and mentee throughout our tenure working together. She is an incredibly strong and talented woman who has been, and continues to be, my role model as I navigate being a scientist and a mother.

I would like to thank my committee members, Geeta Narlikar and Mark Moasser. Both have exceptional critical scientific thinking that has helped direct my work and steer me in a better direction whenever I started to veer off course. I'm especially grateful for Geeta making time to meet with me to help with analysis of my enzyme kinetics data and her clear approach to problem solving. I am especially grateful for Mark's quick critical scientific thinking and his straightforward feedback.

Luckily, science does not occur in a vacuum, and I absolutely could not have accomplished this without the help and support of my wonderful friends and coworkers. Everyone in the Jura lab – past and present – has been awesome to work with. I am so lucky to get to work in a lab where I feel like going to work each day is going to hang out with my friends. I would like to thank Michael Hopkins for making me feel at home in the lab right from the very start and for his sense of humor and his love of 90's rock. I would like to thank Jennifer

Kung for always having a listening ear and continuing to be a voice of reason. Your advice is always exactly what I need to hear. I would like to thank Tarjani Thaker and Christopher Agnew, two awesome postdocs in the lab from whom I have learned so much. Their scientific help has been absolutely invaluable, but their friendship (or frenemy-ship) has been even more so. I'm also grateful for the other graduate students in the lab: Karen Ruiz, Megan Lo, Mitch Lopez, and Devan Diwanji. They always offer a supportive ear when I need to vent and genuinely make the lab a fun and enjoyable place to work. I would like to thank Kelsie Eichel for being my scientific advisor, confidante, and most importantly my closest friend. She has been with me from the beginning of this crazy journey and I would not have made it without her support. I would like to thank two of my dearest friends, Peter Littlefield and Jasmine Kelly-Pierce. I would not have made it in the lab without Peter's scientific help and supportive friendship. Thank you both for going on a milkshake tasting journey which has turned into a lasting friendship.

I would like to thank all of my family. My brother Brian and his family Katy, Leela, and Jolene are the best cheerleaders and although we live far apart, my visits with them always rejuvenate my soul. My mom and dad have always been the most supportive of all of my endeavors, even when it takes me far away. My dad nurtured my love of both science and music on our commute to youth orchestra, listening to the college of class rock knowledge and discussing the cool new science in latest issue of Discover magazine. My mom is the most caring and compassionate person I know. She was somehow able to constantly go above and beyond in supporting my brother and I in school, sports, and music while also going to school and being an amazing role model for continuing to pursue your life goals. It is with a debt of gratitude that can never be repaid that I would like to thank them for always giving me one hundred percent of

their support and providing me with opportunities that they never had – most importantly the opportunity to just be myself, and the opportunity to pursue my dreams whatever they may be.

Lastly, I need to thank my amazing husband Remi and my wonderful son Miles. Remi has earned this as much as I have. He has provided an ear to listen, a shoulder to cry on, brought me food when I needed it, and spent many late nights in lab with me while I was working. He never complained when I said I had to work all weekend or if we had to plan our time around my tissue culture schedule. He was there to celebrate every success no matter how minor, and to support me through every failure. He gave me the freedom to decide whether to quit or keep going, all while steadfastly giving me the courage and fortitude to continue to the end. He embarked on the wild adventure of parenting with me during my time in graduate school and has proven to be an even more amazing father than partner. I need to thank our wonderful son Miles for the joy and love he brings to my life. Watching him grow and experiment with the world around him has renewed my own love of science. Loving someone so intensely has given me a new perspective on how sacred life is and added new purpose to my ultimate scientific mission of discovering new facets of biology and improving human health.

Abstract

Investigating non-canonical mechanisms of receptor tyrosine kinase signaling

by

Nicole Amber Michael Frazier

This thesis examines multiple facets of the human epidermal growth factor receptor-3 (HER3) signaling. Receptor tyrosine kinases are typically activated through ligand-dependent homodimerization resulting in trans-autophosphorylation and subsequent kinase activation, resulting in phosphorylation of tyrosines which serve as recruitment sites for downstream signal transducers. These homomeric interactions are tightly regulated and occur only within RTK sub-families thereby limiting cross-activation between unrelated receptors. HER3 is one of four members of the EGFR/HER family of RTKs, consisting of EGFR, HER2, HER3, and HER4. This family of RTKs is activated through a unique mechanism where ligand binding drives formation of an asymmetric dimer in which one receptor, the “activator”, allosterically activates its partner, the “receiver”. Among this family, HER3 is unique in that it has mutations within several key residues that render it catalytically impaired. In spite of this, HER3 is able to signal by assuming the “activator” role when paired with EGFR, HER2, or HER4, leading to phosphorylation of the HER3 C-terminal tail. The tail of HER3 contains six direct binding sites for phosphatidylinositol-3 kinase (PI3K) recruitment resulting in its exceptional ability to potently activate the PI3K pathway.

The MET receptor, along with the Ron receptor, make up the MET receptor family. Like the HER family, the MET receptor also plays a role in cancer progression particularly in driving invasiveness and metastasis. The most common mechanism of activation of MET in cancer is

through protein overexpression, often through genomic amplification. The MET receptor couples to activation of the MAPK and PI3K pathways through a bidentate binding site in its C-terminal domain which directly recruits Gab1. In cancers with MET overexpression, MET has also been found to drive phosphorylation of multiple other unrelated RTKs.

The first chapter of this thesis elucidates how overexpression of MET in cancer mediates phosphorylation of HER3 in the Golgi apparatus. The second chapter investigates the contributions of individual PI3K binding sites, and describes a new role for SHC, in activation of PI3K/Akt signaling by HER3.

Table of Contents

Chapter 1: Overexpression-mediated activation of MET in the Golgi promotes HER3/ERBB3 phosphorylation	1
1.1 Abstract.....	2
1.2 Introduction.....	4
1.3 Results.....	6
1.4 Discussion.....	15
1.5 Materials and Methods.....	19
1.6 References.....	23
1.7 Figures.....	33
Chapter 2: HER3 potentiates robust PI3K signaling through multiple redundant PI3K binding sites and non-canonical recruitment through SHC	48
2.1 Abstract.....	49
2.2 Introduction.....	50
2.3 Results.....	53
2.4 Discussion.....	61
2.5 Materials and Methods.....	65
2.6 References.....	68
2.7 Figures.....	75

List of Figures

Chapter 1

Figure 1 Overexpression of MET drives HER3 phosphorylation independently of EGFR and HER2.....	38
Figure 2 HER3 interacts specifically with an intracellular pool of MET	39
Figure 3 HER3 and MET co-localize in the Golgi under conditions of MET overexpression.....	40
Figure 4 HER3 phosphorylation in cancer cells with <i>MET</i> amplification is ligand-independent	41
Figure 5 Phosphorylated MET and HER3 localize to the Golgi in cancer cells with <i>MET</i> amplification	42
Figure 6 HER3 phosphorylation contributes to proliferation in MHCC97-H cells.....	43
Figure 7 EGFR is another RTK substrate of MET phosphorylated in the Golgi.....	44
Supplementary Figure 1 Inhibition of MET does not affect interaction with HER3.....	45
Supplementary Figure 2 Inhibition of MET significantly decreases cell proliferation	46
Supplementary Figure 3 MET drives phosphorylation of multiple receptors in MHCC97-H cells	47

Chapter 2

Figure 1 HER3 is unusual among PI3K binding proteins in having six YxxM sites	79
Figure 2 All six YxxM sites in HER3 contribute to PI3K signaling	80
Figure 3 Even in the absence of all YxxM sites, HER3 can maintain Ba/F3 viability.....	81
Figure 4 Recruitment of SHC to HER3 activates PI3K in the absence of YxxM motifs	82

Figure 5 The Y1054 and Y1289 YxxM sites are stronger potentiators of cell survival than the other HER3 YxxM sites.....83

Figure 6 HER3 signals through both the p110 α and p110 β **isoforms** of PI3K84

Figure 7 Evolutionary analysis of YxxM motifs in HER3 suggests Y1054 may be the most conserved in the HER3 tail85

Chapter 1: Overexpression-mediated activation of MET in the Golgi promotes HER3/ERBB3 phosphorylation

This chapter contains a reprint of “Overexpression-mediated activation of MET in the Golgi promotes HER3/ERBB3 phosphorylation” (in revision in *Oncogene*). Nicole Michael Frazier developed the project, conducted most experiments and analysis, and wrote the paper. Toni Brand (Department of Otolaryngology – Head and Neck Surgery, UCSF) conducted PLA experiments. John D. Gordan (Division of Hematology and Oncology – UCSF) provided essential materials. Jennifer Grandis (Department of Otolaryngology – Head and Neck Surgery, UCSF) provided support and scientific guidance. Natalia Jura (Cardiovascular Research Institute, Department of Cellular and Molecular Pharmacology, UCSF) contributed to project development, data analysis, and paper writing.

1.1 ABSTRACT

Ligand-dependent oligomerization of receptor tyrosine kinases (RTKs) results in their activation through highly specific conformational changes in the extracellular and intracellular receptor domains. These conformational changes are unique for each RTK sub-family, limiting cross-activation between unrelated RTKs. The proto-oncogene MET receptor tyrosine kinase overcomes these structural constraints and phosphorylates unrelated RTKs in numerous cancer cell lines. The molecular basis for these interactions is unknown. We investigated the mechanism by which MET phosphorylates the human epidermal growth factor receptor-3 (HER3 or ERBB3), a catalytically impaired RTK whose phosphorylation by MET has been described as an essential component of drug resistance to inhibitors targeting EGFR and HER2. We find that in untransformed cells, HER3 is not phosphorylated by MET in response to ligand stimulation, but rather to increasing levels of MET expression, which results in MET activation in a ligand-independent manner. Phosphorylation of HER3 by its canonical dimerization partners, EGFR and HER2, is achieved by engaging an allosteric site on the HER3 kinase domain, but this site is not required when HER3 is phosphorylated by MET. We also observe that HER3 preferentially interacts with MET during its maturation along the secretory pathway, before MET is post-translationally processed by cleavage within its extracellular domain. This results in accumulation of phosphorylated HER3 in the Golgi apparatus. We further show that in addition to HER3, MET phosphorylates other RTKs in the Golgi, suggesting that this mechanism is not limited to HER3 phosphorylation. These data demonstrate a link between MET overexpression and its aberrant activation in the Golgi endomembranes and suggest that non-canonical interactions between MET and unrelated RTKs occur during maturation of receptors. Our study

highlights a novel aspect of MET signaling in cancer that would not be accessible to inhibition by therapeutic antibodies.

1.2 INTRODUCTION

Under homeostatic conditions the hepatocyte growth factor (HGF) receptor (HGFR/MET) becomes activated by binding to an extracellular ligand, HGF, which induces receptor dimerization, activation of the intracellular tyrosine kinase domains and subsequent receptor phosphorylation.¹⁻⁵ The phosphorylated receptor sites then efficiently recruit downstream signaling adaptors to activate signaling cascades that modulate epithelial cell motility and invasion, formation of branched tubules, and cell growth and survival.⁶⁻⁹ In cancer, aberrant signaling by the MET receptor is primarily achieved by overexpression or amplification of genes encoding *MET* or its ligand, and is associated with tumorigenesis, metastasis, and poor prognosis.¹⁰⁻¹⁷ Hyper-activated MET phosphorylates other RTKs, particularly the EGFR/HER family, often as a mechanism of resistance to targeted therapies.

Phosphorylation of one HER receptor, the catalytically impaired HER3 pseudokinase, has been described as an important mechanism of drug resistance.¹⁸⁻²¹ Under normal conditions, HER3 is phosphorylated by EGFR or HER2, and potently stimulates cell survival through the Akt signaling pathway by direct recruitment of PI3K.^{22, 23} In lung cancer cells with an activating EGFR mutation and acquired resistance to EGFR inhibitors, *MET* amplification can restore HER3 phosphorylation and downstream signaling through the PI3K/Akt pathway.¹⁸ In numerous other cancer cells lines in which MET is overexpressed, HER3 becomes phosphorylated in a MET-dependent manner^{19, 24-27} and was shown to interact with MET by co-immunoprecipitation.^{24, 25, 28} Thus, the ability of MET to phosphorylate HER3 under conditions of overexpression is a well-established phenomenon, however the molecular basis for this non-canonical cross-phosphorylation between RTKs is not understood.

While the mechanisms for activation and phosphorylation remain poorly defined for many RTKs, structural studies on receptors such as EGFR²⁹⁻³³ and the insulin receptor (IR) family³⁴⁻³⁷ have revealed unique protein-protein interactions that are required to trigger kinase activity and are specific for each subfamily of RTKs. In cancers in which MET efficiently phosphorylates other RTKs, these specific mechanisms no longer seem to apply. At present, it is unknown whether the promiscuity with which MET phosphorylates other RTKs reflects an inherent ability to interact directly with these receptors, or if it is only a consequence of overexpression. It is also unclear whether these non-canonical kinase-substrate relationships are mediated by tractable protein-protein interactions that could be explored therapeutically in cancer.

We set out to understand the mechanism of how overexpression of MET leads to phosphorylation of new substrate RTKs by focusing on MET-dependent phosphorylation of HER3. We show that HER3 is a substrate for MET only under conditions of MET overexpression, and that under these circumstances MET phosphorylates HER3 in a ligand-independent manner. HER3 phosphorylation by MET is also independent from its allosteric activator interface which is crucial for HER3 phosphorylation by other HER receptors. Surprisingly, we found that HER3 almost exclusively interacts with and is phosphorylated by MET in endomembranes, primarily the Golgi apparatus, where overexpressed MET accumulates during biosynthesis. Based on these findings, we propose that in *MET*-amplified cells overcrowding of MET molecules in the secretory pathway facilitates its unspecific interactions with other RTKs, resulting in their premature phosphorylation.

1.3 RESULTS

Overexpression of MET drives HER3 phosphorylation independently of EGFR and HER2

To investigate the mechanism by which MET phosphorylates HER3, we used COS7 cells, which do not express detectable levels of endogenous HER3. When HER3 was transfected with its co-receptor HER2 in COS7 cells, HER3 and HER2 phosphorylation could be detected only in the presence of HER3 ligand neuregulin (NRG) (Figure 1a). In contrast, when HER3 was co-expressed with MET, it was phosphorylated independently of NRG stimulation (Figure 1a). Under these conditions, MET was also phosphorylated in COS7 cells in a ligand-independent manner (Figure 1a). To confirm that HER3 phosphorylation is dependent on MET activity, we treated COS7 cells expressing MET and HER3 with a panel of MET inhibitors and found they consistently blocked phosphorylation of both HER3 and MET (Figure 1b).

To test if overexpression of MET is necessary for mediating HER3 phosphorylation, we assessed levels of phosphorylated HER3 in COS7 cells as a function of activation of the endogenous MET by HGF. HER3 phosphorylation was not significantly induced by HGF stimulation over the basal level, despite robust activation of endogenous MET (Figure 1c). We further observed that the extent of HER3 phosphorylation increased linearly with the levels of overexpressed, hyper-activated MET (Figure 1d). These data suggest that HGF-dependent activation of MET is insufficient to stimulate HER3 phosphorylation, and that MET-dependent HER3 phosphorylation only occurs under conditions of MET overexpression.

Since MET has been reported to interact with other members of the EGFR/HER family^{24-26, 38} we looked at whether MET-dependent HER3 phosphorylation is a result of cross-activation of EGFR and/or HER2 by MET. We used lapatinib, a highly selective EGFR and HER2 kinase inhibitor. Lapatinib treatment eliminated HER2-dependent HER3 phosphorylation induced by

NRG stimulation, but had no effect on HER3 phosphorylation that results from MET overexpression (Figure 1e). We also examined phosphorylation of the HER3 variant with a mutation in the allosteric site within the kinase domain (V926R). This variant is unable to form functional dimers with other HER receptors and abolishes NRG-dependent HER3 phosphorylation (Figure 1f).³⁹ Using this mutant, we can test not only whether MET-dependent phosphorylation of HER3 depends on formation of active complexes between HER3 and EGFR or HER2, but also whether HER3 forms structurally similar complexes with MET. As shown in Figure 1e, the HER3 V926R mutant loses the ability to be phosphorylated by HER2 in a NRG-dependent manner, but is phosphorylated by MET to the same extent as wild-type HER3. Together these results demonstrate that MET overexpression induces HER3 phosphorylation independently from activation of other HER receptors and does not engage the allosteric site of HER3.

HER3 interacts specifically with an intracellular pool of MET

To investigate if MET and HER3 interact under conditions of MET-dependent phosphorylation of HER3 in COS7 cells, we immunoprecipitated FLAG-tagged constructs of MET or HER3, transiently co-expressed in COS7 cells with un-tagged versions of HER3 or MET, respectively. As shown in Figure 2a and 2b, FLAG-tagged MET co-immunoprecipitated with un-tagged HER3. Likewise, FLAG-tagged HER3 co-immunoprecipitated with un-tagged MET. These results are consistent with previous observations that MET and HER3 interact in lung cancer cells in which *MET* is amplified.^{18, 38} This interaction was not significantly affected by capmatinib treatment, despite full inhibition of MET and HER3 phosphorylation (Supplementary Figure 1).

The MET receptor is typically resolved as a double band on SDS/PAGE due to a post-translational modification that involves cleavage within the extracellular domain of MET.² This results in an α chain (50 kDa) and β chain (145 kDa) which remain bound together by disulfide linkages.^{40, 41} When these bonds are broken under reducing SDS/PAGE conditions, MET is typically detected as a doublet composed of the immature uncleaved form (170 kDa) and the β chain (145 kDa) (Figure 2c).

Our analysis of the co-immunoprecipitates between MET and HER3 led to a consistent observation that HER3 almost exclusively pulls down the upper band of the MET doublet, corresponding to the uncleaved form of MET (Figure 2c). MET is cleaved by furin or a furin-like protease in the trans-Golgi network during receptor anterograde trafficking to the plasma membrane.⁴² Uncleaved MET is therefore expected to be located primarily in the endomembranes. We separated the plasma membrane and intracellular pools of MET receptor by biotin-labeling surface proteins in COS7 cells expressing MET, and isolating them from intracellular proteins by affinity purification with Neutravidin-agarose beads. As expected, only mature MET (detected as 145 kDa β chain) is labeled with biotin, whereas the uncleaved form of MET, which we find to interact with HER3, is predominantly protected from labeling (Figure 2d). This analysis indicates that under conditions of MET overexpression, the interaction between MET and HER3 does not occur at the plasma membrane but rather in the intracellular membranes.

HER3 and MET co-localize in the Golgi under conditions of MET overexpression

To better understand the spatial determinants of the HER3/MET interaction and resulting HER3 phosphorylation, we used immunofluorescence to determine the localization of phosphorylated

HER3 in COS7 cells under conditions of MET overexpression. In a control experiment, we examined the localization of phosphorylated HER3 in cells that were co-transfected with HER2, serum-starved, and stimulated with NRG. Under these conditions, in more than 80% of cells HER3 phosphorylation could be detected exclusively at the cell periphery, indicative of localization at the plasma membrane (Figure 3a). In contrast, in over 80% of cells co-expressing MET and HER3, HER3 phosphorylation was not detected at the cell periphery, but instead within a perinuclear compartment (Figure 3a). This redistribution of phosphorylated HER3 did not reflect changes in localization of the total HER3 receptor, which was localized both at the cell periphery as well as in the perinuclear compartment (Figure 3a). Notably, in contrast to HER3 and HER2, the overexpressed MET receptor was predominantly detected in the perinuclear compartment (Figure 3a).

To characterize the perinuclear compartment where MET and phosphorylated HER3 are localized, we co-stained COS7 cells expressing MET and HER3 with a set of endomembrane compartment markers, Golgin-97 (Golgi), PDI (endoplasmic reticulum), and EEA1 (early endosomes). The MET and phospho-HER3 signals overlaid most extensively with Golgin-97, with detectable but much less pronounced overlay with PDI and EEA1, demonstrating that a significant pool of phosphorylated HER3 co-localizes with MET in the Golgi (Figure 3b). These data are consistent with the results of the co-immunoprecipitation and surface biotinylation/fractionation analyses and show that under conditions of MET overexpression, HER3 predominantly interacts with MET in Golgi endomembranes.

HER3 phosphorylation in cancer cells with *MET* amplification is ligand-independent

To relate our analysis of HER3/MET interactions in the COS7 cell model system of MET overexpression to a physiological scenario of *MET* amplification, we used a hepatocellular carcinoma cell line, MHCC97-H, in which genomic *MET* is amplified approximately 15-fold.⁴³

⁴⁴ In these cells, MET phosphorylation was constitutive, was not further stimulated upon addition of HGF, and was eliminated upon treatment with a MET inhibitor, capmatinib (Figure 4a).

Notably, in these cells, HER3 was constitutively phosphorylated, and its phosphorylation was significantly diminished by inhibition of MET with capmatinib (Figure 4b). In contrast, lapatinib treatment did not substantially change the extent of HER3 phosphorylation (Figure 4b). These data demonstrate that constitutive phosphorylation of HER3 in MHCC97-H cells is primarily a result of MET activity and not of the activity of the canonical HER3 co-receptors, HER2 and EGFR. To our knowledge, this is the first demonstration of a kinase/substrate relationship between MET and HER3 in cells in which *MET* amplification has not originated as an acquired mechanism of resistance to EGFR or HER2 inhibitors. Our results strengthen the hypothesis that HER3 phosphorylation is a direct consequence of MET overexpression, and can also occur in cancer cells with no documented dependence on EGFR/HER2 receptor signaling for growth.

An interesting and consistent observation we made was a significant increase in HER3 protein levels upon MET inhibition. This phenomenon has been previously noted in cell lines with constitutively activated MET^{24, 45} and was determined to occur at the mRNA level in response to MET inhibition.⁴⁵ We also observed that EGFR was constitutively phosphorylated in MHCC97-H cells, even in the presence of its own potent inhibitor, lapatinib (Figure 4b).

Treatment with capmatinib blocks EGFR phosphorylation, suggesting that, like HER3, EGFR is a substrate of activated MET in MHCC97-H cells. Remarkably, HER2 is not similarly constitutively phosphorylated by MET in MHCC97-H cells (Figure 4b).

We observed a significant number of MET and HER3 interactions through proximity ligation assay (PLA) analysis in MHCC97-H cells, which remained unchanged under different conditions, such as steady state growth media, serum starvation, and stimulation with NRG (Figure 4c). These results are consistent with earlier observations that HER3 phosphorylation by MET is ligand-independent (Figure 4b).

Phosphorylated MET and HER3 localize to the Golgi in cancer cells with *MET* amplification

Next, we used immunofluorescence to detect the location of phosphorylated endogenous receptors in MHCC97-H cells. Both the total and the phosphorylated MET signals were detected at the cell periphery as well as concentrated in a perinuclear compartment, consistent with our observations in COS7 cells (Figure 5a). Treatment with the MET inhibitor, crizotinib, completely eliminated phosphorylated MET signal (Figure 5a). We were unable to detect total endogenous HER3, but were successful in detecting phosphorylated HER3. Although the phospho-HER3 signal was much weaker overall than the signal detected for phosphorylated MET, it could be found both at the cell periphery and at the perinuclear compartment, similar to where phosphorylated MET was found (Figure 5b). This immunofluorescence pattern was eliminated by treatment with crizotinib, but not with the EGFR inhibitor gefitinib (Figure 5b), consistent with our data in Figure 4b that HER3 phosphorylation is MET-dependent. Notably, in MHCC97-H cells we detected more significant localization of phosphorylated HER3 at the cell periphery than we did in COS7 cells in which MET was over-expressed.

To identify the nature of the perinuclear compartment in MHCC97-H cells, we used markers specific for Golgi, ER and early endosomes. Similar to our observations in COS7 cells,

we observed the most extensive co-localization between phosphorylated receptors and Golgin-97 (Figure 5c and 5d). These results demonstrate not only that MET is abundantly present in the Golgi apparatus in cancer cells, but also that this population of MET is activated and co-localizes with phosphorylated HER3.

HER3 phosphorylation contributes to proliferation of MHCC97-H cells

In lung cancer cells resistant to EGFR kinase inhibitors, persistent HER3 phosphorylation is essential for cell survival and dependent on *MET* amplification.¹⁸ While HER3 phosphorylation is a potent activator of the PI3K pathway, and to a smaller extent the MAPK pathway, both of these pathways are also efficiently activated by MET. Because *MET* amplification is the driving oncogenic signal in MHCC97-H cells, we tested whether HER3 phosphorylation is functionally significant in these cells.

As expected, MHCC97-H cells rely on MET signaling, and treatment with capmatinib significantly reduced the proliferation of these cells (Figure 6a). To test the significance of HER3 signaling for MHCC97-H cell proliferation, we used siRNA to knock-down HER3 (Figure 6b). Our initial analysis showed that loss of HER3 had no significant effect on the proliferation of MHCC97-H cells (Figure 6a and 6d). Furthermore, the activation of the PI3K-Akt or MAPK/ERK pathways was not reduced upon HER3 knock-down in MHCC97-H cells (Figure 6c).

We considered possible redundancy between signaling pathways activated by HER3 and other HER receptors and hypothesized that HER3 phosphorylation may be more critical when its close relatives, EGFR and HER2, can no longer efficiently signal. We therefore used lapatinib to inhibit EGFR and HER2. Although in previous experiments we observed that EGFR could still

be phosphorylated in the presence of lapatinib in a MET-dependent manner (Figure 4b), lapatinib treatment is expected to block the ability of EGFR to propagate the signal as the inhibited EGFR will no longer be able to phosphorylate recruited signaling effectors. Indeed, in the presence of lapatinib, HER3 knock-down led to a moderate but significant decrease in cell proliferation to ~70% of control siRNA treated cells (Figure 6d and Supplementary Figure 2). Likewise, in control experiments when cells were treated with capmatinib – which is expected to inhibit all MET-dependent phosphorylation events – knock-down of HER3 made a small but significant impact only in the presence of lapatinib (Figure 6d and Supplementary Figure 2). Unexpectedly, analysis of signaling pathway activation under the same serum-starved conditions as the proliferation assays revealed a resurgence of Akt phosphorylation upon sustained treatment with either lapatinib or capmatinib, which was inhibited with the combination of both inhibitors (Figure 6e). The MAPK/ERK pathway was blocked upon MET inhibition as expected since MET is known to be a strong activator of this pathway. These results suggest that MET-dependent HER3 phosphorylation in MHCC97-H cells plays a functional role in cell proliferation which can be uncovered in the absence of EGFR activation.

EGFR is another RTK substrate of MET phosphorylated in the Golgi

Our data show that MET overexpression in cancer cells results in its premature activation in the Golgi in a ligand-independent manner. Since MET has been previously observed to phosphorylate a broad range of RTKs under conditions of overexpression,^{19, 20, 26, 38} we hypothesized that this apparent promiscuity reflects encounters between newly synthesized RTKs and hyperactivated MET during receptor trafficking to the plasma membrane. To determine if MET also phosphorylates a range of RTKs in *MET*-amplified MHCC97-H cells, we

used an RTK array to analyze the phosphorylation status of 49 different RTKs in MHCC97-H cells grown in the presence of DMSO, capmatinib, or crizotinib under serum-starved conditions. In the DMSO-treated sample, MET was highly phosphorylated along with several other receptors, notably EGFR, HER3, Ret, DDR1, and Ryk. Treatment with capmatinib or crizotinib abolished phosphorylation of MET and all other RTKs, demonstrating that hyperactivation of MET in MHCC97-H cells is coupled to phosphorylation of multiple RTKs (Figure 7a & Supplementary Figure 3).

Among RTK substrates of MET in MHCC97-H cells, EGFR was most potently phosphorylated (Figure 7a). Our results in Figure 4b further show that constitutive EGFR phosphorylation in these cells is largely independent from intrinsic EGFR kinase activity, and is instead dependent on MET. Using immunofluorescence, we also found substantial concentration of phosphorylated EGFR in the Golgi compartment in MHCC97-H cells (Figure 7b). Phospho-EGFR staining was eliminated with capmatinib treatment, but not when cells were treated with the EGFR inhibitor, gefitinib. These data point to a similar mechanism through which MET phosphorylates both EGFR and HER3.

1.4 DISCUSSION

MET-mediated phosphorylation of other RTKs in cancer cells, including EGFR/HER family members, has been reported in numerous malignancies. The mechanisms that allow MET to phosphorylate such a wide spectrum of RTK substrates, which otherwise auto-phosphorylate or are phosphorylated by closely homologous RTK family members, are not understood. Our results describe one mechanism that would allow MET to indiscriminately phosphorylate RTKs through their transient co-localization with hyper-activated MET in the secretory pathway. By focusing our studies on one RTK substrate of MET, HER3, we show that this interaction does not engage molecular interfaces that mediate activation of HER3 by the HER family of receptors.

It is uncertain what leads to intracellular accumulation and activation of overexpressed MET in cancer cells. Following synthesis in the ER, MET undergoes extensive post-translational modification, including N- and O-linked glycosylation, and recently reported palmitoylation.⁴⁶⁻⁴⁸ These modifications are essential for proper MET function, and inhibition of palmitoylation and N-linked glycosylation have both been shown to impair maturation of MET and trafficking to the plasma membrane.^{46, 47} The efficiency of MET progression through the secretory pathway is also regulated by the functions of acid sphingomyelinase (ASM) and syntaxin 6 (STX6), as well as by the levels of cholesterol.⁴⁹ Collectively, these regulatory mechanisms are responsible for the maintenance of an intracellular pool of MET in the Golgi that is used to replenish MET at the plasma membrane.⁴⁹ A perinuclear pool of MET, which primarily consists of de novo synthesized MET, has also been observed in cancer cell models and tumor samples.^{50 51} In cancer cells with MET overexpression, inefficient post-translational modifications might elicit perinuclear accumulation of immature MET receptors – which nevertheless have a functional

kinase domain. Increased local concentration of the kinase domains would then drive receptor activation even in the absence of canonical regulation by ligand binding. One could speculate that cells could mitigate receptor overcrowding by improving the rate of their maturation or alternative mechanisms that would decrease their unspecific interactions. Interestingly, in gastric cancer cells, O-linked glycosylation of MET was shown to negatively regulate MET activation⁴⁸ which could hypothetically entail preventing receptor interactions in the absence of ligand binding.

During biosynthesis, MET is also proteolytically cleaved in the trans-Golgi-network.⁴² Interestingly, an uncleaved variant of MET, p109NC is constitutively activated in LoVo cells.⁵² Although the mechanism through which p190NC is activated is unknown at present, this MET variant is not impaired in trafficking to the plasma membrane. Curiously HER3 is also constitutively phosphorylated in LoVo cells.⁵³ Whether p190NC drives phosphorylation of HER3 and does so through abnormal accumulation in the Golgi, will be an exciting topic for future studies.

Overexpression or mutation of several other RTKs has been shown to impair receptor trafficking to the cell surface resulting in accumulation of an intracellular pool of activated receptors. Specifically, oncogenic mutants of ALK, c-Kit, and Flt3 have all been shown to be retained in the ER and Golgi as a result of their constitutive activation.⁵⁴⁻⁵⁷ Similarly, overexpression of FGFR1 and FGFR2 in COS7 leads to activation of immature receptors at the Golgi apparatus, which still elicit typical downstream signaling responses, such as phosphorylation of downstream effector STAT1.⁵⁸ In the case of Flt3, change in localization qualitatively changes downstream signaling from its typical membrane-localized downstream effectors to acquisition of new substrates.⁵⁹ Hence, accumulation of activated RTKs in

endomembranes can result in a variety of signaling responses from the intracellular compartment. Based on our data we propose that MET-dependent phosphorylation of other RTKs represents yet another example of aberrant signaling resulting from intracellular RTK activation.

Although our studies focus on the functional interaction between MET and HER3, hyperactivated MET facilitates phosphorylation of many unrelated receptors such as EGFR, HER3, Ret, DDR1, and Ryk, in the hepatocellular carcinoma cell line we tested. Previously published RTK array analyses in cell lines from different cancer types have identified largely overlapping sets of RTKs whose phosphorylation becomes MET-dependent.^{19, 20, 26, 38} The EGFR/HER family members are consistently identified as substrates of MET in these analyses, as well as Ret, and the MET-family member Ron. The prominence of the EGFR/HER family as substrates of MET is striking and may reflect the fact that these receptors are themselves potent oncogenes. It is possible that cells under physiological stress, such as MET overexpression, compensate by upregulating multiple signaling pathways, and that the EGFR/HER family is particularly good at supporting cell survival in this context. The additional variation of MET substrates observed in these studies might reflect differential receptor expression levels or be indicative of the unique mechanisms through which different cancers support their survival. The lack of clear substrate specificity further argues that functional interactions between MET and other RTKs do not rely on a common molecular mechanism, but rather are driven by MET overexpression, which turns low affinity, unspecific interactions into productive phosphorylation events before the receptors fully progress through the secretory pathway.

Our results increase a body of evidence supporting the propensity of MET to signal intracellularly, which has also been shown to originate from endosomes^{60, 61} and the nucleus⁶².

⁶³. The endosomal pool of MET originates from the plasma membrane following ligand stimulation and results in perinuclear accumulation of activated MET capable of inducing downstream signaling, such as activation of STAT3.^{60, 61} A truncated and activated form of nuclear MET has been found in both prostate and hepatocellular cancers and linked to activation of a variety of pathways including SRY (sex determining region Y)-box9, β -catenin, and Nanog homeobox, and NF- κ B.^{62, 63} These mechanisms seem to fundamentally differ from how constitutive MET activation is achieved through overexpression during receptor biosynthesis. Collectively, this broad spectrum of intracellular functions of MET has ramifications for antibody-based therapies targeting MET. There are currently numerous antibody therapies targeting MET or its ligand HGF in development and clinical trials,⁶⁴⁻⁶⁹ but these therapies are expected to perform poorly in MET expressing-tumors in which a large population of activated MET is localized intracellularly. Thus far, anti-MET antibody therapies appear to have fallen short of their potential in clinical trials with the absence of a significant clinical benefit to patients.⁶⁴⁻⁶⁷ Our finding that a large population of MET can be activated in the Golgi could help account for these lackluster results and adds weight to the notion that combining small molecule with antibody therapies could more effectively target tumors with this phenotype.

1.5 MATERIALS AND METHODS

Cell Culture

MHCC97-H cells were obtained from the Liver Cancer Institute and Zhongshan Hospital of Fudan University, Shanghai. COS7 cells are a monkey kidney fibroblast-like cell line obtained from Dr. John Kuriyan at UC-Berkeley. COS7 and MHCC97-H cells were cultured in DMEM supplemented with 10% FBS and streptomycin/penicillin. Inhibitor assays were treated for 6-24 hours in serum-free media containing capmatinib/INCB28060 (Selleckchem), crizotinib/PF-02341066 (Selleckchem), gefitinib/ZD1839 (Selleckchem), or lapatinib.

Transfection

COS7 cells were transfected using FuGene6 (Promega) and cultured for 24-48 hours. MHCC97-H cells were reverse transfected with non-targeting (Dharmacon siGENOME Non-Targeting siRNA Pool#1: UAGCGACUAAACACAUCAA, UAAGGCUAUGAAGAGAUAC, AUGUAUUGGCCUGUAUUAG, AUGAACGUGAAUUGCUCAA) or HER3 siRNA (Dharmacon siGENOME Human ERBB3 (2065) siRNA: GCAGUGGAUUCGAGAAGUG, AGAUUGUGCUCACGGGACA, GUGGAUUCGAGAAGUGACA, GCCGAUGCUGAGAACCAAUA) using Lipofectamine RNAiMax.

Western blotting

Cells were lysed in lysis buffer (50mM Tris pH 7.5, 150mM NaCl, 1mM EDTA, 1mM Na₃VO₄, 1mM NaF, 1% Triton X-100), or RIPA buffer (50mM Tris pH 7.5, 150mM NaCl, 1mM EDTA, 1mM Na₃VO₄, 1mM NaF, 0.1% SDS, 0.1% deoxycholate, 1% IGEPAL CA-630) with protease inhibitor cocktail (Roche). Lysates were run on 8 or 10% SDS-PAGE and transferred to PVDF

membrane (EMD Millipore). Proteins were detected using: anti-MET (D1C2 XP– Cell Signaling), anti-phospho-MET Tyr1234/Y1235 (Cell Signaling), anti-HER3 (SC-285 – Santa Cruz), anti-HER3 (SC-81455 – Santa Cruz), anti-HER3 (D22C5 XP – Cell Signaling), anti-phospho-HER3 Tyr1289 (21D3 – Cell Signaling), anti-HER2 (SC-284 – Santa Cruz), anti-phospho-HER2 Tyr1221/1222 (Cell Signaling), anti-FLAG M2 (Sigma-Aldrich), anti-EGFR ((1005) SC-03 – Santa Cruz), anti-phospho-EGF-Receptor Tyr1068 (Cell Signaling), β -tubulin (9F3 – Cell Signaling). Secondary antibodies were anti-rabbit-IgG HRP-linked antibody (Cell Signaling), or anti-mouse IgG HRP-linked whole antibody (GE Healthcare Biosciences). Blots were developed using ECL/ECL Prime (Thermo Fisher Scientific).

Immunoprecipitation

Cells were lysed, cleared by centrifugation, and incubated with anti-FLAG-M2 antibody (Sigma Aldrich #F1804) for 2-12 hours at 4C followed by incubation with 1:1 protein A-sepharose slurry (Life Technologies). Immunoprecipitates were analyzed by western blotting.

Immunofluorescence

3×10^6 cells were plated on coverslips. After 24 hours, cells were transfected and cultured for 24-48 hours. Cells were fixed with 3.7% formaldehyde for 1 hour at room temperature, permeabilized with 0.1% Triton X-100 for 5 minutes, and blocked with 1% BSA for 5 minutes. Cells were incubated with primary antibodies at 37C for 1-2 hours: anti-FLAG-M2 antibody (Sigma Aldrich #F1804), anti-phospho-HER3 Tyr1289 (21D3 – Cell Signaling), anti-MET (D1C2 – Cell Signaling), anti-phospho-MET Tyr1234/Y1235 (Cell Signaling), anti-phospho-EGF-Receptor Tyr1068 (Cell Signaling), anti-Golgin97 (A-21270 – Molecular Probes), anti-PDI

(RL90 - Thermo Scientific), or anti-EEA1 (BD Biosciences - 610456). Cells were washed and incubated with fluorescently tagged anti-rabbit or anti-mouse secondary antibodies (Goat Anti-Mouse Alexa-fluor-568 cat#A11031; Alexa-Fluor-488 donkey anti-rabbit cat# A21206 – Life technologies). Images were taken at 60x magnification using a Nikon widefield epifluorescent microscope.

Phospho-RTK Array

Phosphorylated RTKs were identified from MHCC97-H cells using the Proteome Profiler Human Phospho-RTK Array Kit (R&D Systems ARY001B). Cells were treated with DMSO, crizotinib, or capmatinib, for 24 hours in serum-free media. Cells were lysed and protein concentration was standardized by Bradford assay. Samples were incubated on the array membrane overnight at 4C. Membranes were washed and phosphorylated receptors were detected using HRP-conjugated phosphotyrosine antibody.

Proliferation assay

After 24 hours transfection with siRNA, cells were serum-starved +/-drug and cultured for 48 hours. Cells were washed, incubated with crystal violet solution (0.5% crystal violet, 25% methanol) for 10 minutes, washed, and dried overnight. Dye was solubilized in 1:1 ethanol:sodium citrate solution for 1 hour, transferred to 96-well plate, and absorbance was read at 595nm.

Proximity Ligation Assay

MHCC97-H cells were grown on four-well chamber slides and processed using the Duolink In Situ Fluorescence kit with red detection reagents (Sigma-Aldrich) per the manufacturer's instructions. MET (D1C2 XP– Cell Signaling) and HER3 G4 (SC-203) primary antibodies were used.

Statistics

Sample sizes were chosen to be sufficient to obtain reliable results consistent with standard practices within this field. Statistics were determined and displayed using Excel (Microsoft, Redmond, WA). Results represent an average of at least three independent experiments and exact sample size is noted in figure legends. Data are presented as mean \pm SEM for co-localization and proximity ligation assay analysis, and as grand mean \pm pooled standard deviation for proliferation assay analysis. The variances within each group of compared data were similar in almost all cases, and all were well within one order of magnitude. For proliferation assay analysis, two treatments were compared by unpaired two-tailed *t*-tests, determined to have normal distributions by Shapiro-Wilk test, and p-values below 0.05 were considered significant.

1.6 REFERENCES

- 1 Park M, Dean M, Kaul K, Braun MJ, Gonda MA, Vande Woude G. Sequence of MET protooncogene cDNA has features characteristic of the tyrosine kinase family of growth-factor receptors. *Proc Natl Acad Sci U S A* 1987; 84: 6379-6383.
- 2 Gherardi E, Youles ME, Miguel RN, Blundell TL, Iamele L, Gough J *et al.* Functional map and domain structure of MET, the product of the c-met protooncogene and receptor for hepatocyte growth factor/scatter factor. *Proc Natl Acad Sci U S A* 2003; 100: 12039-12044.
- 3 Bottaro DP, Rubin JS, Faletto DL, Chan AM, Kmieciak TE, Vande Woude GF *et al.* Identification of the hepatocyte growth factor receptor as the c-met proto-oncogene product. *Science* 1991; 251: 802-804.
- 4 Chirgadze DY, Hepple JP, Zhou H, Byrd RA, Blundell TL, Gherardi E. Crystal structure of the NK1 fragment of HGF/SF suggests a novel mode for growth factor dimerization and receptor binding. *Nat Struct Biol* 1999; 6: 72-79.
- 5 Rodrigues GA, Park M. Autophosphorylation modulates the kinase activity and oncogenic potential of the Met receptor tyrosine kinase. *Oncogene* 1994; 9: 2019-2027.
- 6 Zhu H, Naujokas MA, Fixman ED, Torossian K, Park M. Tyrosine 1356 in the carboxyl-terminal tail of the HGF/SF receptor is essential for the transduction of signals for cell motility and morphogenesis. *J Biol Chem* 1994; 269: 29943-29948.

- 7 Ponzetto C, Bardelli A, Maina F, Longati P, Panayotou G, Dhand R *et al.* A novel recognition motif for phosphatidylinositol 3-kinase binding mediates its association with the hepatocyte growth factor/scatter factor receptor. *Mol Cell Biol* 1993; 13: 4600-4608.
- 8 Ponzetto C, Bardelli A, Zhen Z, Maina F, dalla Zonca P, Giordano S *et al.* A multifunctional docking site mediates signaling and transformation by the hepatocyte growth factor/scatter factor receptor family. *Cell* 1994; 77: 261-271.
- 9 Bladt F, Riethmacher D, Isenmann S, Aguzzi A, Birchmeier C. Essential role for the c-met receptor in the migration of myogenic precursor cells into the limb bud. *Nature* 1995; 376: 768-771.
- 10 Song Z, Wang X, Zheng Y, Su H, Zhang Y. MET Gene Amplification and Overexpression in Chinese Non-Small-Cell Lung Cancer Patients Without EGFR Mutations. *Clin Lung Cancer* 2017; 18: 213-219 e212.
- 11 Christensen JG, Burrows J, Salgia R. c-Met as a target for human cancer and characterization of inhibitors for therapeutic intervention. *Cancer Lett* 2005; 225: 1-26.
- 12 Li A, Niu FY, Han JF, Lou NN, Yang JJ, Zhang XC *et al.* Predictive and prognostic value of de novo MET expression in patients with advanced non-small-cell lung cancer. *Lung Cancer* 2015; 90: 375-380.
- 13 Li Y, Li W, He Q, Xu Y, Ren X, Tang X *et al.* Prognostic value of MET protein overexpression and gene amplification in locoregionally advanced nasopharyngeal carcinoma. *Oncotarget* 2015; 6: 13309-13319.

- 14 Yan S, Jiao X, Zou H, Li K. Prognostic significance of c-Met in breast cancer: a meta-analysis of 6010 cases. *Diagn Pathol* 2015; 10: 62.
- 15 Casadevall D, Gimeno J, Clave S, Taus A, Pijuan L, Arumi M *et al.* MET expression and copy number heterogeneity in nonsquamous non-small cell lung cancer (nsNSCLC). *Oncotarget* 2015; 6: 16215-16226.
- 16 Dimou A, Non L, Chae YK, Tester WJ, Syrigos KN. MET gene copy number predicts worse overall survival in patients with non-small cell lung cancer (NSCLC); a systematic review and meta-analysis. *PLoS One* 2014; 9: e107677.
- 17 Seiwert TY, Jagadeeswaran R, Faoro L, Janamanchi V, Nallasura V, El Dinali M *et al.* The MET receptor tyrosine kinase is a potential novel therapeutic target for head and neck squamous cell carcinoma. *Cancer Res* 2009; 69: 3021-3031.
- 18 Engelman JA, Zejnullahu K, Mitsudomi T, Song Y, Hyland C, Park JO *et al.* MET amplification leads to gefitinib resistance in lung cancer by activating ERBB3 signaling. *Science* 2007; 316: 1039-1043.
- 19 Kataoka Y, Mukohara T, Tomioka H, Funakoshi Y, Kiyota N, Fujiwara Y *et al.* Foretinib (GSK1363089), a multi-kinase inhibitor of MET and VEGFRs, inhibits growth of gastric cancer cell lines by blocking inter-receptor tyrosine kinase networks. *Invest New Drugs* 2012; 30: 1352-1360.
- 20 Kim SM, Kim H, Yun MR, Kang HN, Pyo KH, Park HJ *et al.* Activation of the Met kinase confers acquired drug resistance in FGFR-targeted lung cancer therapy. *Oncogenesis* 2016; 5: e241.

- 21 Stommel JM, Kimmelman AC, Ying H, Nabioullin R, Ponugoti AH, Wiedemeyer R *et al.* Coactivation of receptor tyrosine kinases affects the response of tumor cells to targeted therapies. *Science* 2007; 318: 287-290.
- 22 Soltoff SP, Carraway KL, 3rd, Prigent SA, Gullick WG, Cantley LC. ErbB3 is involved in activation of phosphatidylinositol 3-kinase by epidermal growth factor. *Mol Cell Biol* 1994; 14: 3550-3558.
- 23 Kim HH, Sierke SL, Koland JG. Epidermal growth factor-dependent association of phosphatidylinositol 3-kinase with the erbB3 gene product. *J Biol Chem* 1994; 269: 24747-24755.
- 24 Liu X, Wang Q, Yang G, Marando C, Koblisch HK, Hall LM *et al.* A novel kinase inhibitor, INCB28060, blocks c-MET-dependent signaling, neoplastic activities, and cross-talk with EGFR and HER-3. *Clin Cancer Res* 2011; 17: 7127-7138.
- 25 Guo A, Villen J, Kornhauser J, Lee KA, Stokes MP, Rikova K *et al.* Signaling networks assembled by oncogenic EGFR and c-Met. *Proc Natl Acad Sci U S A* 2008; 105: 692-697.
- 26 Agarwal S, Zerillo C, Kolmakova J, Christensen JG, Harris LN, Rimm DL *et al.* Association of constitutively activated hepatocyte growth factor receptor (Met) with resistance to a dual EGFR/Her2 inhibitor in non-small-cell lung cancer cells. *Br J Cancer* 2009; 100: 941-949.
- 27 Shi P, Oh YT, Zhang G, Yao W, Yue P, Li Y *et al.* Met gene amplification and protein hyperactivation is a mechanism of resistance to both first and third generation EGFR inhibitors in lung cancer treatment. *Cancer Lett* 2016; 380: 494-504.

- 28 Yun C, Gang L, Rongmin G, Xu W, Xuezhi M, Huanqiu C. Essential role of Her3 in two signaling transduction patterns: Her2/Her3 and MET/Her3 in proliferation of human gastric cancer. *Mol Carcinog* 2015; 54: 1700-1709.
- 29 Zhang X, Gureasko J, Shen K, Cole PA, Kuriyan J. An allosteric mechanism for activation of the kinase domain of epidermal growth factor receptor. *Cell* 2006; 125: 1137-1149.
- 30 Jura N, Endres NF, Engel K, Deindl S, Das R, Lamers MH *et al.* Mechanism for activation of the EGF receptor catalytic domain by the juxtamembrane segment. *Cell* 2009; 137: 1293-1307.
- 31 Garrett TP, McKern NM, Lou M, Elleman TC, Adams TE, Lovrecz GO *et al.* Crystal structure of a truncated epidermal growth factor receptor extracellular domain bound to transforming growth factor alpha. *Cell* 2002; 110: 763-773.
- 32 Dawson JP, Berger MB, Lin CC, Schlessinger J, Lemmon MA, Ferguson KM. Epidermal growth factor receptor dimerization and activation require ligand-induced conformational changes in the dimer interface. *Mol Cell Biol* 2005; 25: 7734-7742.
- 33 Ferguson KM, Berger MB, Mendrola JM, Cho HS, Leahy DJ, Lemmon MA. EGF activates its receptor by removing interactions that autoinhibit ectodomain dimerization. *Mol Cell* 2003; 11: 507-517.
- 34 Kavran JM, McCabe JM, Byrne PO, Connacher MK, Wang Z, Ramek A *et al.* How IGF-1 activates its receptor. *Elife* 2014; 3.

- 35 Menting JG, Whittaker J, Margetts MB, Whittaker LJ, Kong GK, Smith BJ *et al.* How insulin engages its primary binding site on the insulin receptor. *Nature* 2013; 493: 241-245.
- 36 Favelyukis S, Till JH, Hubbard SR, Miller WT. Structure and autoregulation of the insulin-like growth factor 1 receptor kinase. *Nat Struct Biol* 2001; 8: 1058-1063.
- 37 McKern NM, Lawrence MC, Streltsov VA, Lou MZ, Adams TE, Lovrecz GO *et al.* Structure of the insulin receptor ectodomain reveals a folded-over conformation. *Nature* 2006; 443: 218-221.
- 38 Tanizaki J, Okamoto I, Sakai K, Nakagawa K. Differential roles of trans-phosphorylated EGFR, HER2, HER3, and RET as heterodimerisation partners of MET in lung cancer with MET amplification. *Br J Cancer* 2011; 105: 807-813.
- 39 Jura N, Shan Y, Cao X, Shaw DE, Kuriyan J. Structural analysis of the catalytically inactive kinase domain of the human EGF receptor 3. *Proc Natl Acad Sci U S A* 2009; 106: 21608-21613.
- 40 Tempest PR, Stratton MR, Cooper CS. Structure of the met protein and variation of met protein kinase activity among human tumour cell lines. *Br J Cancer* 1988; 58: 3-7.
- 41 Stamos J, Lazarus RA, Yao X, Kirchhofer D, Wiesmann C. Crystal structure of the HGF beta-chain in complex with the Sema domain of the Met receptor. *EMBO J* 2004; 23: 2325-2335.

- 42 Komada M, Hatsuzawa K, Shibamoto S, Ito F, Nakayama K, Kitamura N. Proteolytic processing of the hepatocyte growth factor/scatter factor receptor by furin. *FEBS Lett* 1993; 328: 25-29.
- 43 Tang ZY, Ye SL, Liu YK, Qin LX, Sun HC, Ye QH *et al.* A decade's studies on metastasis of hepatocellular carcinoma. *J Cancer Res Clin Oncol* 2004; 130: 187-196.
- 44 Du Z, Caenepeel S, Shen Y, Rex K, Zhang Y, He Y *et al.* Preclinical Evaluation of AMG 337, a Highly Selective Small Molecule MET Inhibitor, in Hepatocellular Carcinoma. *Mol Cancer Ther* 2016; 15: 1227-1237.
- 45 Steinway SN, Dang H, You H, Rountree CB, Ding W. The EGFR/ErbB3 Pathway Acts as a Compensatory Survival Mechanism upon c-Met Inhibition in Human c-Met+ Hepatocellular Carcinoma. *PLoS One* 2015; 10: e0128159.
- 46 Chen R, Li J, Feng CH, Chen SK, Liu YP, Duan CY *et al.* c-Met function requires N-linked glycosylation modification of pro-Met. *J Cell Biochem* 2013; 114: 816-822.
- 47 Coleman DT, Gray AL, Kridel SJ, Cardelli JA. Palmitoylation regulates the intracellular trafficking and stability of c-Met. *Oncotarget* 2016; 7: 32664-32677.
- 48 Liu SY, Shun CT, Hung KY, Juan HF, Hsu CL, Huang MC *et al.* Mucin glycosylating enzyme GALNT2 suppresses malignancy in gastric adenocarcinoma by reducing MET phosphorylation. *Oncotarget* 2016; 7: 11251-11262.
- 49 Zhu L, Xiong X, Kim Y, Okada N, Lu F, Zhang H *et al.* Acid sphingomyelinase is required for cell surface presentation of Met receptor tyrosine kinase in cancer cells. *J Cell Sci* 2016; 129: 4238-4251.

- 50 Ruco LP, Ranalli T, Marzullo A, Bianco P, Prat M, Comoglio PM *et al.* Expression of Met protein in thyroid tumours. *J Pathol* 1996; 180: 266-270.
- 51 Kermorgant S, Zicha D, Parker PJ. Protein kinase C controls microtubule-based traffic but not proteasomal degradation of c-Met. *J Biol Chem* 2003; 278: 28921-28929.
- 52 Mondino A, Giordano S, Comoglio PM. Defective posttranslational processing activates the tyrosine kinase encoded by the MET proto-oncogene (hepatocyte growth factor receptor). *Mol Cell Biol* 1991; 11: 6084-6092.
- 53 Beji A, Horst D, Engel J, Kirchner T, Ullrich A. Toward the prognostic significance and therapeutic potential of HER3 receptor tyrosine kinase in human colon cancer. *Clin Cancer Res* 2012; 18: 956-968.
- 54 Mazot P, Cazes A, Bouterin MC, Figueiredo A, Raynal V, Combaret V *et al.* The constitutive activity of the ALK mutated at positions F1174 or R1275 impairs receptor trafficking. *Oncogene* 2011; 30: 2017-2025.
- 55 Bougherara H, Subra F, Crepin R, Tauc P, Auclair C, Poul MA. The aberrant localization of oncogenic kit tyrosine kinase receptor mutants is reversed on specific inhibitory treatment. *Mol Cancer Res* 2009; 7: 1525-1533.
- 56 Tabone-Eglinger S, Subra F, El Sayadi H, Alberti L, Tabone E, Michot JP *et al.* KIT mutations induce intracellular retention and activation of an immature form of the KIT protein in gastrointestinal stromal tumors. *Clin Cancer Res* 2008; 14: 2285-2294.

- 57 Schmidt-Arras DE, Bohmer A, Markova B, Choudhary C, Serve H, Bohmer FD. Tyrosine phosphorylation regulates maturation of receptor tyrosine kinases. *Mol Cell Biol* 2005; 25: 3690-3703.
- 58 Citores L, Bai L, Sorensen V, Olsnes S. Fibroblast growth factor receptor-induced phosphorylation of STAT1 at the Golgi apparatus without translocation to the nucleus. *J Cell Physiol* 2007; 212: 148-156.
- 59 Choudhary C, Olsen JV, Brandts C, Cox J, Reddy PN, Bohmer FD *et al.* Mislocalized activation of oncogenic RTKs switches downstream signaling outcomes. *Mol Cell* 2009; 36: 326-339.
- 60 Kermorgant S, Parker PJ. Receptor trafficking controls weak signal delivery: a strategy used by c-Met for STAT3 nuclear accumulation. *J Cell Biol* 2008; 182: 855-863.
- 61 Lefebvre J, Ancot F, Leroy C, Muharram G, Lemiere A, Tulasne D. Met degradation: more than one stone to shoot a receptor down. *FASEB J* 2012; 26: 1387-1399.
- 62 Xie Y, Lu W, Liu S, Yang Q, Carver BS, Li E *et al.* Crosstalk between nuclear MET and SOX9/beta-catenin correlates with castration-resistant prostate cancer. *Mol Endocrinol* 2014; 28: 1629-1639.
- 63 Tey SK, Tse EYT, Mao X, Ko FCF, Wong AST, Lo RC *et al.* Nuclear Met promotes hepatocellular carcinoma tumorigenesis and metastasis by upregulation of TAK1 and activation of NF-kappaB pathway. *Cancer Lett* 2017; 411: 150-161.
- 64 Kim KH, Kim H. Progress of antibody-based inhibitors of the HGF-cMET axis in cancer therapy. *Exp Mol Med* 2017; 49: e307.

- 65 Dieras V, Campone M, Yardley DA, Romieu G, Valero V, Isakoff SJ *et al.* Randomized, phase II, placebo-controlled trial of onartuzumab and/or bevacizumab in combination with weekly paclitaxel in patients with metastatic triple-negative breast cancer. *Ann Oncol* 2015; 26: 1904-1910.
- 66 Shah MA, Bang YJ, Lordick F, Alsina M, Chen M, Hack SP *et al.* Effect of Fluorouracil, Leucovorin, and Oxaliplatin With or Without Onartuzumab in HER2-Negative, MET-Positive Gastroesophageal Adenocarcinoma: The METGastric Randomized Clinical Trial. *JAMA Oncol* 2017; 3: 620-627.
- 67 Shah MA, Cho JY, Tan IB, Tebbutt NC, Yen CJ, Kang A *et al.* A Randomized Phase II Study of FOLFOX With or Without the MET Inhibitor Onartuzumab in Advanced Adenocarcinoma of the Stomach and Gastroesophageal Junction. *Oncologist* 2016; 21: 1085-1090.
- 68 Rosen LS, Goldman JW, Algazi AP, Turner PK, Moser B, Hu T *et al.* A First-in-Human Phase I Study of a Bivalent MET Antibody, Emibetuzumab (LY2875358), as Monotherapy and in Combination with Erlotinib in Advanced Cancer. *Clin Cancer Res* 2017; 23: 1910-1919.
- 69 Cignetto S, Modica C, Chiriaco C, Fontani L, Milla P, Michieli P *et al.* Dual Constant Domain-Fab: A novel strategy to improve half-life and potency of a Met therapeutic antibody. *Mol Oncol* 2016; 10: 938-948.

1.7 FIGURES

Figure 1.

Overexpression of MET drives HER3 phosphorylation independently of EGFR and HER2. **(a)** COS7 cells expressing either MET or HER2 with HER3 were stimulated +/- NRG (50ng/mL) and assayed for HER3 phosphorylation by western blot. **(b)** COS7 cells expressing MET and HER3 were treated with DMSO, or MET inhibitor (1 μ M crizotinib, 100nM capmatinib, 100nM cabozantinib, or 1 μ M merestinib) and assayed for MET and HER3 phosphorylation by western blot. **(c)** COS7 cells expressing HER3 were stimulated with either NRG (50ng/mL), HGF (50ng/mL), or both, and assayed for HER3 phosphorylation by western blot. **(d)** COS7 cells were transiently transfected with HER3 and increasing amounts of MET and assayed for HER3 phosphorylation and MET expression by western blot. **(e)** COS7 cells expressing either HER3 + HER2 or HER3 + MET were treated +/- NRG (50ng/mL) and +/- 3 μ M lapatinib and assayed for HER3 phosphorylation by western blot. **(f)** COS7 cells expressing either wild-type (WT) or V926R mutant (VR) HER3 together with HER2 or MET were stimulated +/- NRG (50ng/mL) and assayed for HER3 phosphorylation.

Figure 2.

HER3 interacts specifically with an intracellular pool of MET. **(a)** COS7 cells expressing MET and FLAG-tagged HER3 were immunoprecipitated with anti-FLAG antibody and assayed for HER3 and MET by western blot. **(b)** COS7 cells expressing HER3 and FLAG-tagged MET were immunoprecipitated with anti-FLAG antibody and assayed for HER3 and MET by western blot. **(c)** Schematic of cleaved and uncleaved MET protein. COS7 cells expressing MET and FLAG-tagged HER3 were immunoprecipitated for anti-FLAG and assayed for MET by western blot. **(d)**

Membrane and intracellular fractions of COS7 cells expressing MET were isolated by surface biotinylation followed by pull-down with Neutravidin-agarose beads and assayed by western blot.

Figure 3.

HER3 and MET co-localize in the Golgi under conditions of MET overexpression. **(a)** COS7 cells expressing HER2-FLAG or MET-FLAG together with HER3-GFP were fixed and stained with anti-FLAG, and anti-phospho-HER3 to visualize HER3 phosphorylation. Localization of HER3 phosphorylation was scored as either membrane, intracellular, or both membrane and intracellular, for 119 cells in the HER3 + MET (-NRG) treatment, 91 cells in the HER3 + MET (+NRG) treatment, 165 cells in the HER3 + HER2 (-NRG) treatment, and 157 cells in the HER3 + HER2 (+NRG) treatment, pooled from a minimum of three experiments and presented as percent of total cells \pm SEM. **(b)** COS7 cells expressing HER3 and MET-BFP were fixed and stained for phospho-HER3 and PDI (ER), EEA1 (early endosome), or Golgin97 (Golgi) markers. Scale bars are 50 μ M.

Figure 4.

HER3 phosphorylation in cancer cells with *MET* amplification is ligand-independent. **(a)** MHCC97-H cells were treated +/- HGF (50ng/mL) and +/- MET inhibitor (100nM capmatinib) and assayed for MET activation by western blotting for phospho-MET. **(b)** MHCC97-H cells were treated with MET inhibitor (100nM capmatinib), EGFR/HER inhibitor (3 μ M lapatinib), or both, and assayed for phosphorylation of MET, HER3, EGFR, and HER2 by western blot. **(c)**

MET and HER3 interactions were assessed in MHCC97-H cells via PLA. Red dots were counted in over 40 nuclei for the no primary control, 64 nuclei for the -NRG treatment, and 49 nuclei for the +NRG treatment, from three or four independent fields of view per treatment and data presented are means \pm SEM.

Figure 5.

Phosphorylated MET and HER3 localize to the Golgi in cancer cells with *MET* amplification. **(a)** MHCC97-H cells were treated +/- MET inhibitor (1 μ M crizotinib), fixed, and stained for MET or phospho-MET. **(b)** MHCC97-H cells were treated with EGFR inhibitor (10 μ M gefitinib), or MET inhibitor (1 μ M crizotinib), then fixed and stained for phospho-HER3. **(c)** MHCC97-H cells were fixed and stained for phospho-MET and PDI (ER), EEA1 (early endosome), or Golgin97 (Golgi) markers. **(d)** MHCC97-H cells were fixed and stained for phospho-HER3 and Golgin97 (Golgi). Scale bars are 50 μ M.

Figure 6.

HER3 phosphorylation contributes to proliferation of MHCC97-H cells. **(a)** MHCC97-H cells were transfected with either non-targeting or HER3 siRNA for 72 hours, treated +/- 100nM capmatinib for 48 hours, and assayed for cell survival using crystal violet staining. Samples were measured in triplicate for three independent experiments. *** $P < 0.0001$ **(b)** MHCC97-H cells were transfected with either non-targeting or HER3 siRNA for 72 hours and assayed for HER3 knock-down by western blot. **(c)** MHCC97-H cells were transfected with either non-targeting or HER3 siRNA for 72 hours and assayed for activation of phospho-HER3, phospho-Akt and

phospho-ERK by western blot. **(d)** MHCC97-H cells were transfected with either non-targeting or HER3 siRNA for 72 hours, treated -/+ 3 μ M lapatinib, 100nM capmatinib, or both for 48 hours, and assayed for cell proliferation using crystal violet staining. Samples were measured in triplicate for three independent experiments and significance determined by two-tailed *t*-test. ** $P < 0.001$, * $P < 0.05$. **(e)** MHCC97-H cells were transfected with either non-targeting or HER3 siRNA for 72 hours, treated -/+ lapatinib, capmatinib, or both for 48 hours, and assayed for activation of signaling pathways by western blot.

Figure 7.

EGFR is another RTK substrate of MET phosphorylated in the Golgi. **(a)** MHCC97-H cells were treated -/+MET inhibitor (100nM capmatinib) and assayed for RTK phosphorylation using phospho-RTK array. **(b)** MHCC97-H cells were treated with EGFR inhibitor (10 μ M gefitinib), or MET inhibitor (100nM capmatinib), then fixed and stained for phospho-EGFR. Scale bars are 50 μ M.

Supplementary Figure 1.

Inhibition of MET does not affect interaction with HER3. **(a)** COS7 cells expressing HER3 alone or together with FLAG-tagged MET were treated -/+ MET inhibitor (100nM capmatinib), immunoprecipitated with anti-FLAG antibody, and assayed by western blot.

Supplementary Figure 2.

Inhibition of MET significantly decreases cell proliferation. **(a)** Differential analysis of data shown in Figure 6d normalized to vehicle control (DMSO) rather than siControl. MHCC97-H cells were transfected with either non-targeting or HER3 siRNA for 72 hours, treated +/- 3 μ M lapatinib, 100nM capmatinib, or both for 48 hours, and assayed for cell proliferation using crystal violet staining. Samples were measured in triplicate for three independent experiments.

Supplementary Figure 3

MET drives phosphorylation of multiple receptors in MHCC97-H cells. **(a)** MHCC97-H cells were treated +/-MET inhibitor (1 μ M crizotinib) and assayed for RTK phosphorylation using phospho-RTK array.

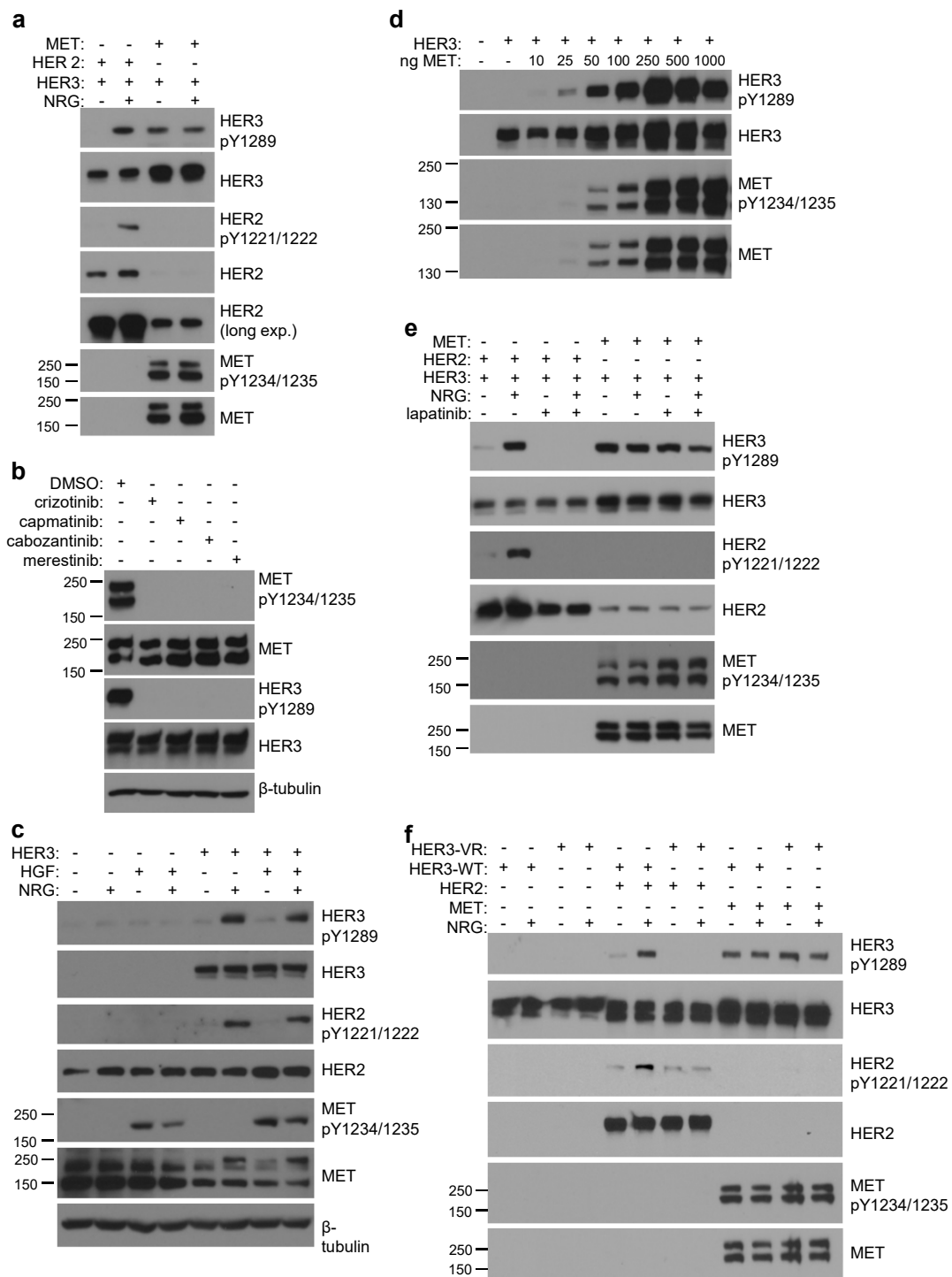


Figure 1. Overexpression of MET drives HER3 phosphorylation independently of EGFR and HER2

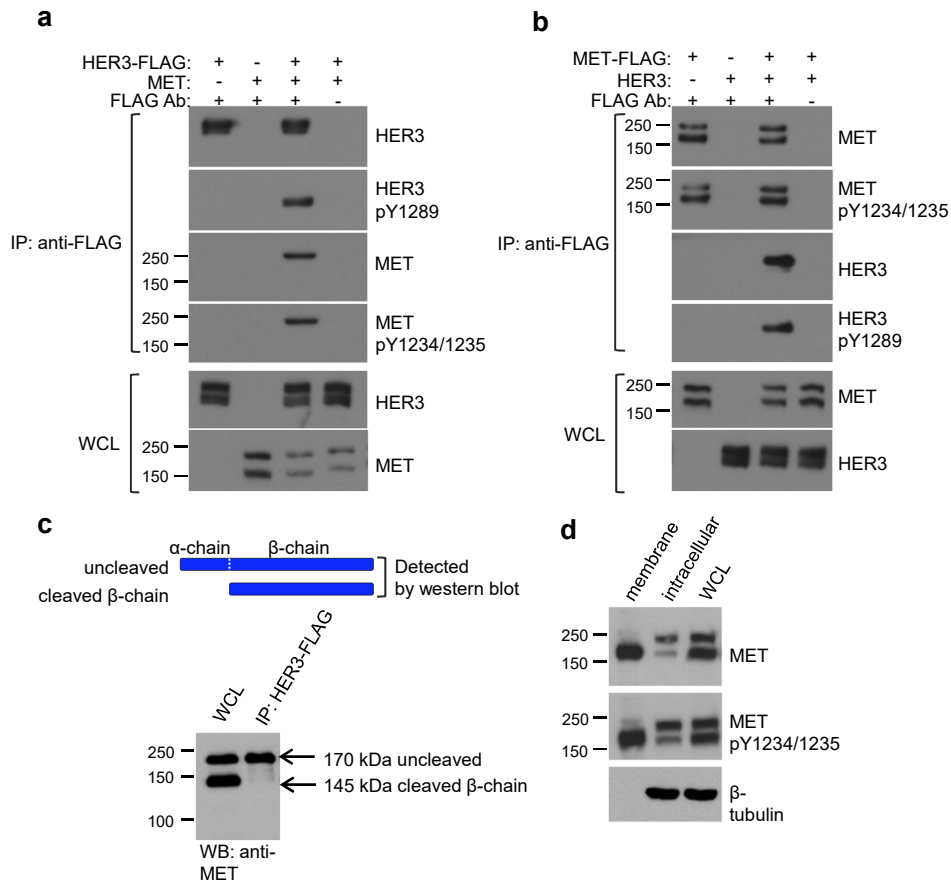


Figure 2. HER3 interacts specifically with an intracellular pool of MET.

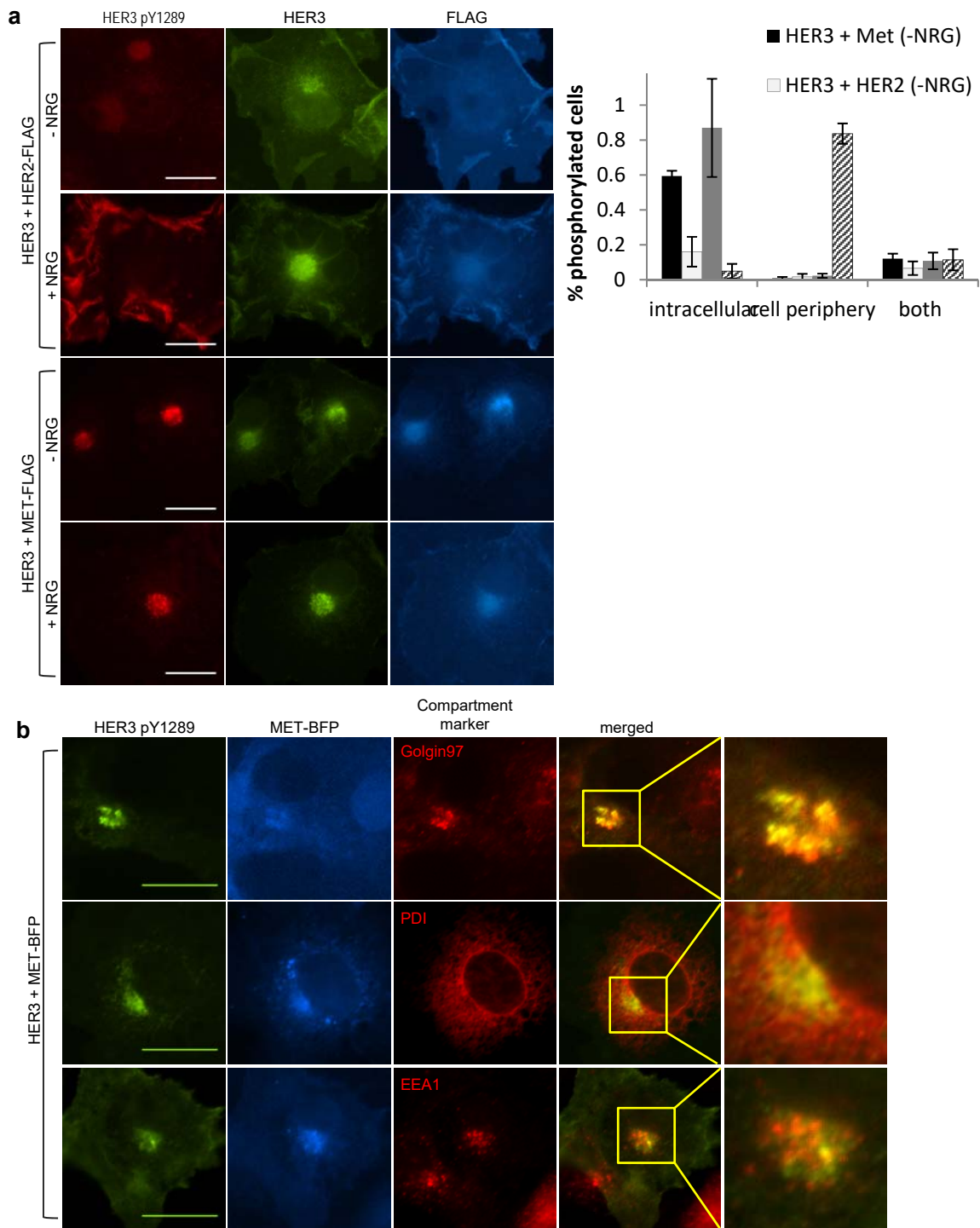


Figure 3. HER3 and MET co-localize in the Golgi under conditions of MET overexpression.

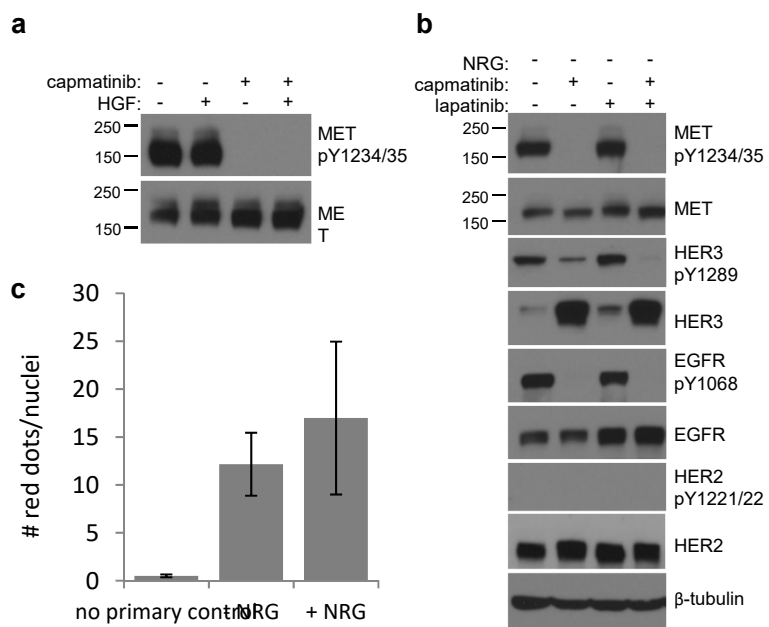


Figure 4. HER3 phosphorylation in cancer cells with MET amplification is ligand-independent

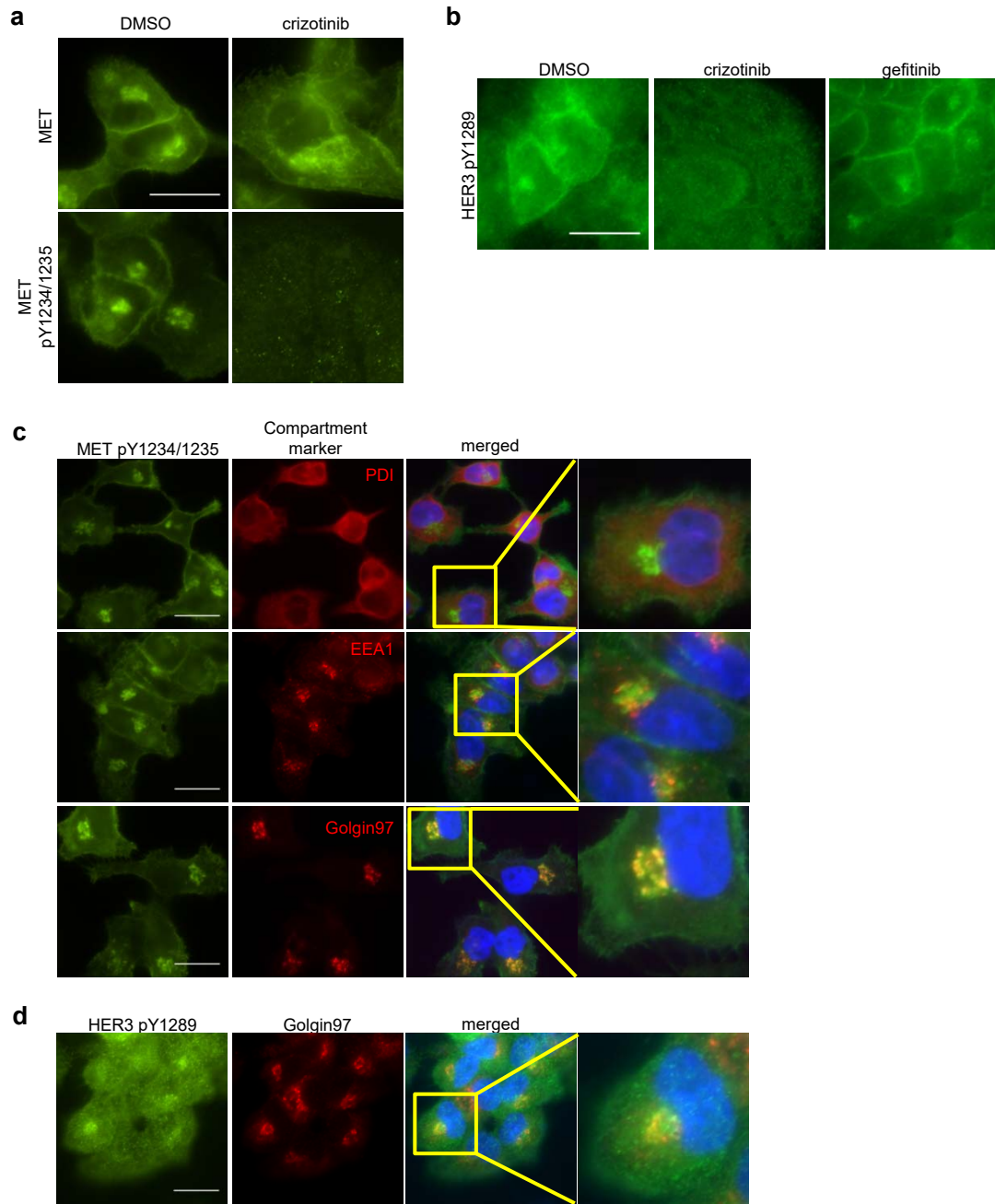


Figure 5. Phosphorylated MET and HER3 localize to the Golgi in cancer cells with MET amplification.

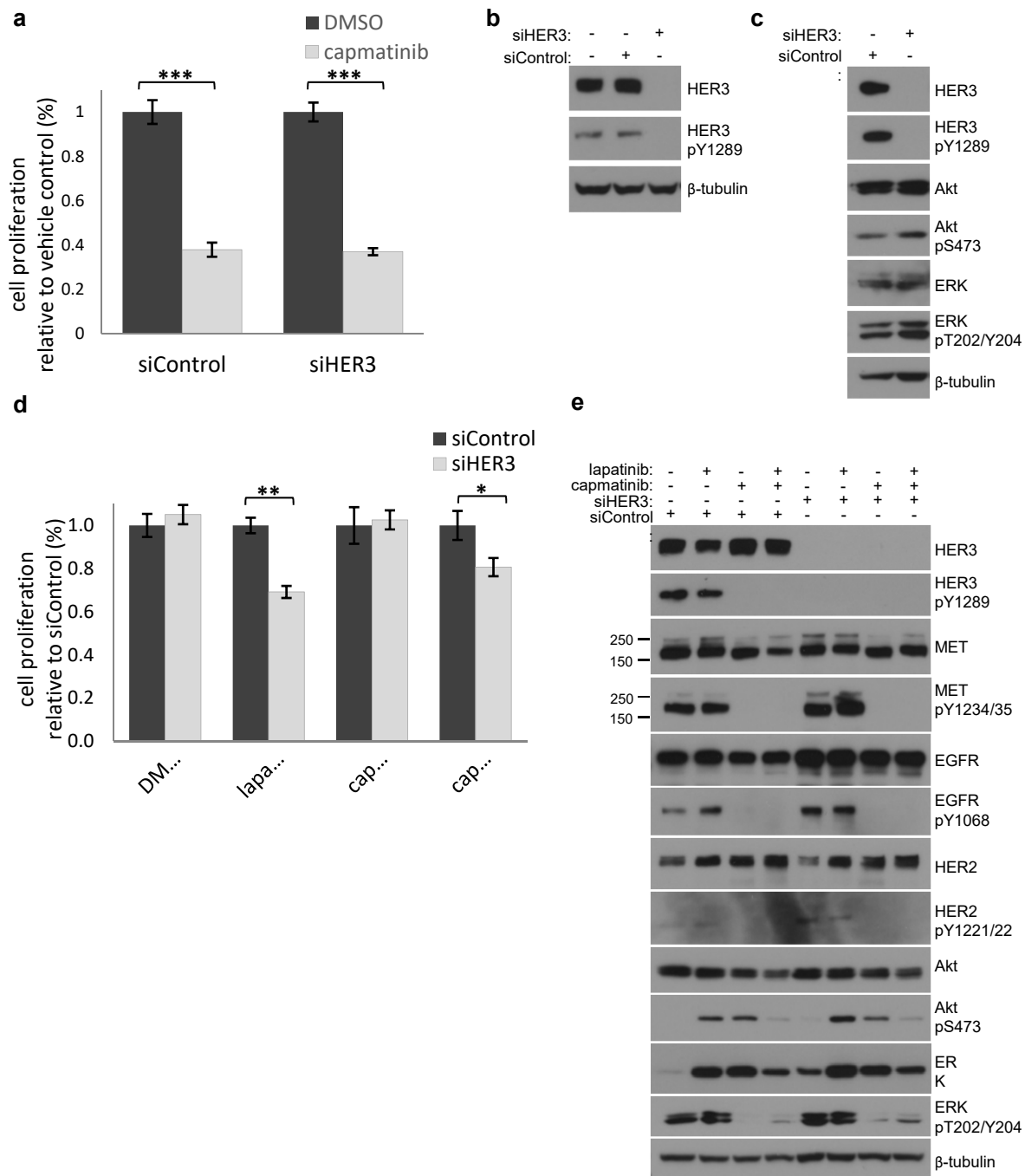


Figure 6. HER3 phosphorylation contributes to proliferation in MHCC97-H cells.

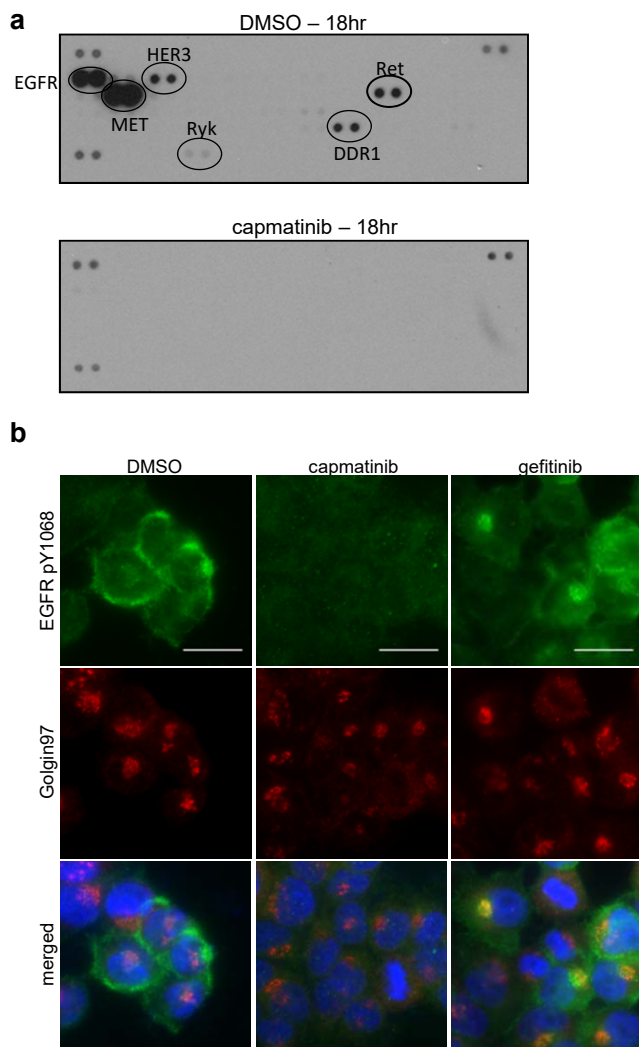
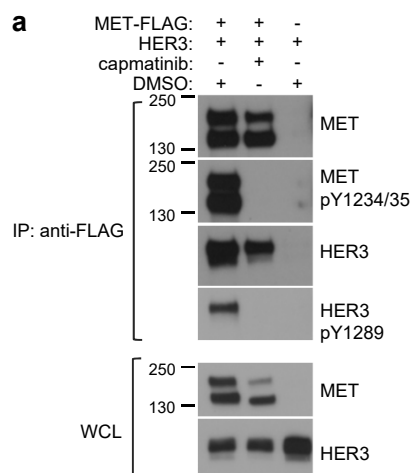
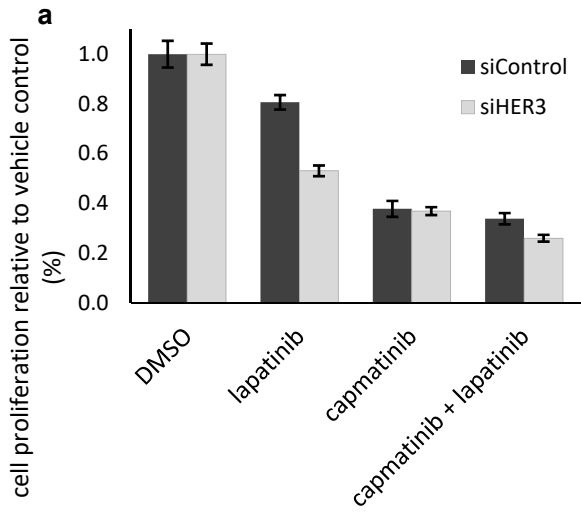


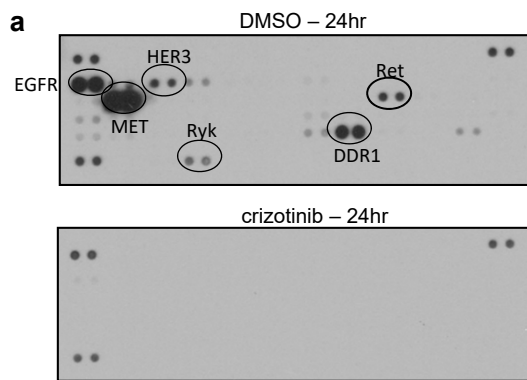
Figure 7. EGFR is another RTK substrate of MET phosphorylated in the Golgi.



Supplementary Figure 1. Inhibition of MET does not affect interaction with HER3



Supplementary Figure 2. Inhibition of MET significantly decreases cell proliferation.



Supplementary Figure 3. MET drives phosphorylation of multiple receptors in MHCC97-H cells.

Chapter 2: HER3 potentiates robust PI3K signaling through multiple redundant PI3K binding sites and non-canonical recruitment through Shc

Nicole Michael Frazier contributed to project development, cloned DNA constructs and generated cell lines, conducted experiments and analysis, and wrote the paper. Michael Hopkins (Cardiovascular Research Institute, UCSF; currently at Verily Life Sciences) originated the project, cloned many DNA constructs and generated cell lines, and conducted experiments and analysis. Krzysztof Pawlowski (Department of Experimental Design and Bioinformatics, Warsaw University of Life Sciences) conducted evolutionary analysis and generated sequence logos. Natalia Jura (Cardiovascular Research Institute, Department of Cellular and Molecular Pharmacology, UCSF) contributed to project development, data analysis, and paper writing.

2.1 ABSTRACT

Phosphorylation of the catalytically impaired human epidermal growth factor receptor-3 (HER3) receptor tyrosine kinase by other members of the HER receptor family enables its function as a versatile scaffold and couples HER3 to activation of the Akt and MAPK signaling pathways. HER3 has evolved to be a particularly powerful activator of the PI3K/Akt pathway due to the presence of six direct binding sites for PI3K in its intracellular tail. This property of HER3 makes it a potent contributor to HER-receptor dependent transformation, as well as an important component of resistance to therapeutics that target other upstream activators of the PI3K pathway or the PI3K pathway itself. It remains unclear what the advantage of multiple recruitment sites might be for activation of the PI3K pathway. To investigate how the individual PI3K binding sites cooperate to control the strength with which HER3 activates the PI3K/Akt pathway, we set up a system in which cell survival is dependent on the activation of the PI3K pathway by HER3. We found that the PI3K binding sites in HER3 are redundant in their ability to activate Akt and that no single site is essential for downstream signaling. Surprisingly, we also discovered that elimination of all six direct binding sites for PI3K on HER3 did not completely block the ability of HER3 to activate the Akt pathway and support cellular survival. In this case, we found that HER3 was able to also indirectly recruit PI3K through interaction with Shc, as mutation of all YxxM sites combined with mutation of the Shc binding site was able to significantly reduce cell survival. Finally, in the context of mutation of the Shc site combined with mutation of all but a single YxxM site, we determined that one site in particular, Y1054, was superior than the rest in driving cell survival. This is potentially linked to its ability to recruit multiple isoforms of PI3K, unlike the other sites which exhibit a strong dependence on the p110-alpha PI3K isoform.

2.2 INTRODUCTION

The human epidermal growth factor receptor (HER) family of receptor tyrosine kinases (RTKs) includes four members: EGFR/HER1, HER2, HER3, and HER4¹⁻⁵. The catalytically impaired HER3, is efficiently phosphorylated by a partner kinase through heterodimer formation with other HER family members⁶ and then acts as a scaffold to coordinate recruitment of downstream signaling transducers. Despite its lack of catalytic activity⁷, HER3 is an extremely powerful activator of the phosphatidylinositol-3 kinase (PI3K) signaling pathway due to the presence of six direct PI3K binding sites within the intracellular tail of HER3^{8,9}. In order to restrain this powerful signaling capacity of HER3, the HER family has developed the unique regulatory feature of separating catalytic activity from the scaffolding function of HER3¹⁰.

PI3K is activated through recruitment of its p85 regulatory subunit to phosphorylated YxxM (Tyr-xxx-xxx-Met) motifs in growth factor receptors and signaling adaptor proteins located at the plasma membrane¹¹. The binding of the SH2 domains of the p85 regulatory subunit to these tyrosines¹²⁻¹⁴ relieves inhibition of the p110 catalytic subunit which can then phosphorylate the membrane lipid phosphatidylinositol 4,5-bisphosphate (PIP2) to phosphatidylinositol 3,4,5-triphosphate (PIP3)^{15,16}. PIP3 is a second messenger which recruits Akt and phosphoinositide-dependent kinase 1 (PDK1) to initiate the Akt signaling cascade to drive cell survival and proliferation^{17,18}.

Activation of the PI3K pathway leads to robust activation of cellular survival and proliferation, thus hyperactivation of PI3K signaling, through HER3 or alone, is a major driver in the development of many cancers¹⁹.

A single YxxM motif is sufficient to activate PI3K signaling, as most signaling molecules which directly bind PI3K contain only 1-2 YxxM motifs. It is then curious that HER3 has

evolved so many PI3K recruitment sites and how each of these individual YxxM motifs in the HER3 tail contribute to activation of PI3K signaling remains undefined. In this study, we set out to understand how these multiple PI3K recruitment sites work together to control the strength with which HER3 activates the PI3K/Akt pathway. We developed a model system in which Ba/F3 cell survival, which is dependent on interleukin-3 (IL-3) signaling, becomes dependent instead on HER3 signaling. We show that HER3 is able to drive IL-3-independent Ba/F3 cell survival in the presence of HER2 as a dimerization partner and neuregulin (NRG) and that this survival is dependent on signaling through PI3K. Mutation of individual YxxM sites to FxxM has no impact on the ability of HER3 to promote cell survival, and conversely, a single YxxM site in the context of all other sites mutated to FxxM is sufficient to promote cell survival, although not to the level of wild-type HER3. Unexpectedly, a negative control with all six YxxM site-tyrosines mutated to FxxM, (referred to as Y6F), was able to strongly promote Ba/F3 cell survival even in the absence of YxxM sites. This effect was also dependent on signaling through PI3K, but not on MAPK signaling. Co-immunoprecipitation and western blot analysis revealed that the Y6F mutant retained a low level of PI3K recruitment and activation of Akt. We found that this residual Akt phosphorylation and subsequent cell survival was due to PI3K recruitment to HER3 through Shc. Blocking Shc binding to HER3 through mutation of the consensus NPDY (Asn-Pro-Asp-Tyr) binding motif in the HER3 tail was able to decrease levels of Akt phosphorylation and cell survival compared to the levels observed with the Y6F mutant. When looking at individual sites in the context of Y6F combined with mutation of the Shc site, two of the sites stand out as superior at driving cell survival than the rest: Y1054 and Y1289. We also found that while all six sites were unaffected by treatment with a PI3K p110 β -specific inhibitor, only Y1054 was also unaffected by treatment with a PI3K p110 α -specific inhibitor, indicating

that only Y1054 has the ability to redundantly recruit either the alpha or beta isoforms. Based on these findings, we hypothesize that Y1054 may be the preferred site of PI3K recruitment to HER3 and the other YxxM sites contribute to amplifying the overall strength of PI3K activation by HER3.

2.3 RESULTS

HER3 is unusual among PI3K binding proteins in having six YxxM sites

Phosphatidylinositol-3 kinase (PI3K) is activated through recruitment to phosphorylated YxxM motifs on signal transducing proteins at the plasma membrane. Many receptor tyrosine kinases have direct binding sites for PI3K while other proteins require adaptor scaffolds to recruit PI3K. In order to better understand the context of PI3K recruitment to HER3, we first analyzed the occurrence of direct PI3K binding sites within the human genome. We limited this analysis to 86 RTKs and signaling adaptor proteins which are validated in the literature to directly bind PI3K. We found that over 90% of proteins analyzed have three or fewer YxxM sites. The majority of direct binders of PI3K contain only a single YxxM motif (57%), while many others contain either two or three YxxM sites (21% and 14%, respectively). HER3 is unique in encoding six YxxM motifs for directly binding PI3K, and is only surpassed by insulin receptor substrate-1 (IRS-1) and IRS-2, which contain 7-9 sites depending on the isoform²⁰ (Figure 1A).

All six YxxM motifs in HER3 contribute to cell survival signaling

We first wanted to investigate the function of each of the individual YxxM sites. Previous work had determined that each site in HER3 was able to bind to and activate PI3K²¹, but how well each of these sites contributes to the biological outcome of cell survival remains unknown. We investigated this by setting up a system in which we could test the function of each of these YxxM sites independently using flow cytometry. Ba/F3 cell survival is dependent on interleukin-3(IL-3) signaling, but can become dependent instead on a different oncogenic signal such as growth factor signaling provided through oncogenic mutation or addition of growth factor to the

growth medium^{22,23}. These cells do not endogenously express HER-family receptors, thus any HER3-driven signaling detected is due to exogenously provided receptors. We created stable Ba/F3 cell lines expressing HER2-GFP and HER3-mCherry variants singly or together. We used a construct of HER2 lacking the C-terminal tail for all of these assays (HER2- Δ tail-GFP) to prevent signaling from HER2, such that only HER3 could activate PI3K signaling. We first assessed whether reconstitution of HER2/HER3 signaling could drive IL-3-independent Ba/F3 survival using flow cytometry to assess cell viability. Cells were counted and resuspended in media lacking IL-3, treated with the HER3 ligand neuregulin (NRG), and viability was assessed every 24 hours for three days. Viability of parental Ba/F3 cells decreased almost to zero 24 hours after IL-3 removal. Likewise, cells expressing only HER2- Δ tail-GFP or HER3-mCherry were non-viable by three days post IL-3 removal. In the absence of NRG, cells co-expressing HER2 and HER3 together were also non-viable and only when these receptors were expressed together and stimulated with the HER3 ligand cells retained greater than 80% viability (Figure 2A). To assess whether this cell viability was dependent upon HER3 activation of PI3K signaling, we treated HER2+HER3-expressing cells with a pan-PI3K inhibitor PIK90 or GDC0941 and assessed viability (Figure 2B and 2C). After 24 hours treatment, HER2+HER3 cell viability was dramatically decreased while in contrast parental Ba/F3 cells were only moderately affected by PI3K inhibition (Figure 2B), demonstrating that HER2+HER3 cells require signaling through PI3K to maintain cell viability. To probe the function of each individual YxxM site within the HER3 tail, we designed multiple series' of HER3 constructs with mutations targeting the YxxM motifs: a negative control construct with each tyrosine in the six YxxM sites mutated to phenylalanine, referred to as Y6F; a set of constructs in the background of Y6F with a single wildtype YxxM while the other five sites are phenylalanine, (FxxM), referred to as single site

knock-In's; and a set of constructs referred to as single site-knock Out's with only a single YxxM motif tyrosine mutated to phenylalanine at a time (Figure 2D). First, we assessed cell viability in cells stably expressing single site knock-In or single site knock-Out constructs. Each of the single site knock-In constructs was sufficient to promote cell survival, although to a lesser degree than wildtype HER3, but to an extent greater or equal to the negative control HER3-Y6F (Figure 2E). Mutation of a single YxxM motif as tested by the single site knock-Out constructs, had no effect on cell viability in comparison to wildtype (Figure 2F). These data suggest that all six YxxM motifs contribute to survival signaling in cells and that there is not a single main PI3K recruitment site responsible for the majority of signaling from HER3.

Even in the absence of all YxxM sites, HER3 can maintain Ba/F3 cell viability

In our initial analysis of the contributions of single YxxM sites in the HER3 tail, we unexpectedly discovered that our negative control HER3-Y6F cells were able to strongly promote cell survival, although to a lesser extent than wildtype HER3 (Figure 3A). Since the HER3 tail encodes thirteen tyrosines within its C-terminal tail, we hypothesized that this residual survival may be due to activation of another signaling pathway. HER3 has been shown to activate MAPK signaling through direct recruitment of Shc to a consensus motif in the C-terminal tail of HER3²⁴. We tested whether this residual survival signaling was dependent on either PI3K or MAPK signaling by treating HER3-Y6F-expressing Ba/F3 cells with a PI3K inhibitor (PIK90) or a MEK1 inhibitor (PD98059). Surprisingly, both wildtype HER3 and HER3-Y6F cells exhibited sensitivity to PI3K inhibition, but were largely unaffected by inhibition of the MAPK pathway (Figure 3B). This implies that HER3-Y6F is still able to activate PI3K signaling to promote cell survival even in the absence of YxxM motifs. To further

test this, we immunoprecipitated HER3 from Ba/F3 cells stably expressing wildtype HER3 or HER3-Y6F following serum starvation and stimulation with NRG. As shown in (Figure 3C), wildtype HER3 strongly pulled down the regulatory p85 subunit of PI3K and the p110 α catalytic subunit, as well as the p110 β , and p110 δ catalytic subunits to a lesser extent. This corresponded to strong downstream phosphorylation of Akt. HER3-Y6F was also able to weakly pull down the p85 regulatory subunit and p110 α catalytic subunits, and exhibited a detectable albeit weak level of Akt phosphorylation (Figure 3C). Since this analysis was performed under the condition of acute ligand stimulation, we next wanted to determine the pattern of Akt and Erk activation under conditions of chronic ligand stimulation, mirroring conditions used in the viability assays. Wildtype HER3 was able to stimulate strong phosphorylation of Akt after five minute acute stimulation on day 1 which was steadily maintained throughout the four-day timecourse (Figure 3D). HER3-Y6F was only able to weakly drive Akt phosphorylation upon initial stimulation, but interestingly this level of phosphorylation increased almost to those seen with wildtype HER3 over the four-day timecourse (Figure 3D). Phosphorylation of Erk1/2 peaked upon initial stimulation and decreased over the length of the timecourse similarly for both wildtype HER3 and HER3-Y6F (Figure 3D). These results taken together suggest that HER3 is capable of activating PI3K signaling in the absence of direct recruitment sites, and that although weak, this signaling is sufficient to promote cell survival.

Recruitment of Shc to HER3 activates PI3K in the absence of YxxM motifs

To understand how HER3 is able to activate PI3K in the absence of YxxM sites, we divided the tail into four approximately equal regions to map where this activity was located in HER3. We created cell lines expressing HER3 with either a single region (referred to as $\Delta 1$, $\Delta 2$, $\Delta 3$, or $\Delta 4$)

or the full C-terminal tail deleted in the background of HER3-Y6F (Figure 4A). Full deletion of the C-terminal tail of HER3 completely eliminated the viability of cells expressing this mutant (Figure 4A), indicating that the ability of HER3-Y6F to promote cell survival was indeed dependent on HER3 and specifically on a site within the C-terminal tail. Deletion constructs $\Delta 1$, $\Delta 2$, or $\Delta 3$ did not affect cell viability, however the $\Delta 4$ deletion construct, decreased cell viability to similar levels as the full tail deletion, signifying that the ability of HER3-Y6F to drive cell survival is located in region 4 of the C-terminal tail (Figure 4A). Region 4 of the C-terminal tail includes two additional tyrosines in addition to three YxxM sites. One of these tyrosines, Y1328, is contained within a Shc consensus binding motif that has been shown to be necessary to activate the MAPK pathway through HER3²⁴, while the other, Y1307, has an unknown function. Shc is typically linked to activation of the MAPK pathway, although there are few reports of Shc activating PI3K signaling^{25, 26}. In order to test if recruitment of Shc to HER3 was responsible for activating PI3K in HER3-Y6F cells, we mutated this tyrosine to phenylalanine (referred to as Y1328F), and first confirmed that this mutation does indeed block binding of Shc to HER3 using immunoprecipitation. Wildtype HER3 and HER3-Y6F both strongly coimmunoprecipitated Shc upon NRG stimulation, while mutation of the Shc site alone or in combination with Y6F completely abrogated the interaction of Shc with HER3 (Figure 4B). Next, we assessed whether combining the Shc site mutation with Y6F was able to eliminate the substantial cell viability observed in HER3-Y6F cells. The Shc site mutation alone had no effect on cell viability relative to wildtype HER3, however the combined mutant of HER3-Y6F-Y1328F had dramatically decreased viability relative to HER3-Y6F, indicating that in HER3-Y6F, the Shc site is able to substantially promote cell survival and that blocking this site is able to block this cell survival (Figure 4C). Correspondingly, we observed that expression of a Y1328F mutation in

combination with HER3-Y6F fully eliminates the weak levels of Akt phosphorylation detected with expression of the HER3-Y6F mutant in HEK293 cells (Figure 4D).

The Y1054 and Y1289 YxxM sites are stronger potentiators of cell survival than the other HER3 YxxM sites

Our initial analysis of single YxxM site function found that all sites were capable of supporting cell survival to a similar degree. However, this was complicated by the strong contribution to cell survival signaling by Shc recruitment to HER3. We therefore theorized that perhaps in the absence of Shc recruitment, we could better discern the relative signaling strengths of individual YxxM sites. To do this we made single knock-In constructs in the background of Y6F-Y1328F, where all sites were mutated to phenylalanine except for a single site (Figure 5A). Ba/F3 cells stably expressing HER2- Δ tail with single-knock-In-Y1328F HER3 constructs were counted and incubated in media lacking IL-3 and supplemented with 25ng/mL NRG. At twenty-four, forty-eight, and seventy-two hours we assessed viability using Sytox blue dead-cell stain and analyzing by flow cytometry. Similar to the previous results, all sites were competent to promote cell survival, but in this case, Y1054 and Y1289 emerged as better than the other sites, with Y1054 being the best (Figure 5B and Figure 5C). This indicates that there are differences between the six YxxM sites in their intrinsic ability to activate PI3K in cells.

HER3 signals through both the p110 α and p110 β isoforms of PI3K

There are multiple isoforms of class I PI3K's which are recruited to RTKs. The majority of RTKs recruit the p85 isoform of the regulatory subunit, and either p110 α , p110 β , or p110 δ isoforms of the catalytic subunit¹¹. The insulin receptor substrate (IRS-1) is a well-studied

example which preferentially recruits and signals through the p110 α isoform²⁷. We hypothesized that perhaps HER3 instead signals through multiple PI3K isoforms and that this could possibly account for the differences in strength between Y1054 and Y1289 and the remaining YxxM sites. To test this, we treated Ba/F3 cells stably expressing wildtype HER3 with inhibitors specific to the p110 α (BH9) and p110 β (TGX-221) isoforms of PI3K and assessed cell viability. These cells were partially sensitive to inhibition of either the p110 α or p110 β isoforms, and treatment with both inhibitors together fully eliminated cell survival over the timecourse (Figure 6A). This illustrates that unlike IRS1, the multiple YxxM sites of HER3 utilize both the p110 α and p110 β isoforms of PI3K to drive cell survival. We next wanted to ask whether different YxxM sites in the HER3 tail had preferences for either the p110 α or p110 β isoform. To do this, we used our single site knock-In-Y1328F constructs, containing all but a single YxxM site and the Shc site mutated, and performed viability assays in the presence of either DMSO, TGX-221, or BH9. Wildtype HER3 was not significantly sensitive to either inhibitor, indicating the intrinsic redundancy of being able to signal through multiple isoforms (Figure 6B). Interestingly, Y1054 was also not significantly sensitive to either inhibitor, suggesting that this site itself is able to recruit both the p110 α and the p110 β isoforms of PI3K. The Y1289 site was slightly sensitive to p110 α inhibition but not significantly to p110 β , suggesting that this site may be able to recruit both isoforms but have a preference for p110 α . The remaining four YxxM sites were all significantly inhibited by p110 α inhibition with greater than 50% inhibition relative to DMSO treatment and only slightly affected by p110 β inhibition (Figure 6B). These data indicate that these four sites, Y1197, Y1222, Y1260, and Y1276, have a strong preference for signaling through the p110 α isoform of PI3K.

Evolutionary analysis of YxxM motifs in HER3 suggests Y1054 may be the most conserved of the six YxxM motifs

We next turned to evolutionary analysis of YxxM sites in HER3 to learn whether the redundancy of having multiple YxxM motifs in HER3 is limited to mammals or vertebrates, or whether this is a more ancient phenomenon. We also wanted to ask whether Y1054 may be the most conserved ancestral site and whether this could account for its unique ability to activate multiple PI3K isoforms. We first analyzed one hundred amino acid sequences of HER3 orthologues from the Uniprot database to determine the frequency of the number of YxxM motifs. The majority (64%) of HER3 orthologues analyzed, contained six sites, and many others contained four or five sites (20% and 12% respectively) (Figure 7A). Of the species that had only 1-3 sites, many of these contained the site homologous to Y1054. An interesting example of this is in zebrafish which encode for three HER3 isoforms containing two, three, or four YxxM motifs. The motif each of these has in common however is the site analogous to Y1054. Next, we generated sequence logos of the HER3 tail restricted to mammalian HER3 orthologues or to vertebrate non-mammalian HER3 orthologues to analyze conservation of YxxM motifs among HER3 orthologues. All six YxxM motifs as well as the Shc NPDY binding motif are very well conserved among mammalian orthologues (Figure 7B). The HER3 tail is much more divergent among non-mammalian vertebrate orthologues, although most YxxM motifs as well as the Shc binding motif are still relatively well conserved. Among both of these groups, Y1054 does appear to be the most conserved (Figure 7B).

2.4 DISCUSSION

Upon initial discovery of HER3 as an EGFR family member, it was hypothesized that HER3 signaling would mimic that of EGFR. However, it was determined that HER3 differs from EGFR in that it does not signal through PLC γ and is instead a significantly stronger activator of the PI3K signaling pathway ultimately leading to a differential effect on phosphorylation of downstream substrates²⁸, and this is due to the presence of the six YxxM motifs within the intracellular C-terminal tail of HER3. Each of these six YxxM motifs is able to associate with the regulatory p85 subunit in a yeast two-hybrid assay²⁹. Our study builds on a previous study in the literature conducting an initial investigation on the role of these individual YxxM sites in activation of PI3K signaling²¹. They found that each site was capable of activating PI3K activity to differential abilities. Specifically, they found that Y1054 and Y1197 pulled down more PI3K activity than the other four sites. Examination of three pairwise combinations of sites for cooperativity in PI3K activation revealed that sites distant from one another did not display cooperativity, while sites within twenty residues were cooperative in their activation of PI3K. They further showed that activation of Akt was dependent on intact YxxM motifs within the HER3 tail. Our study is able to more precisely examine the role of these individual sites due to performing the experiments in the Ba/F3 cells which do not express endogenous HER family proteins. We also go one step further in elucidating how activation of PI3K translates into biological outcomes. Our study confirms their result that the Y1054 site is unique, in that it is the strongest activator of PI3K signaling, and our data suggest that this may be linked to the ability of Y1054 to recruit both the alpha and beta p110 catalytic isoforms.

However, there are a number of other possible reasons for the observed differential abilities of specific YxxM sites to activate PI3K which remain unexamined. The six YxxM sites

in the tail of HER3 differ somewhat in their sequence (Figure 7C). This could itself contribute to different strengths in PI3K activation, as it has been shown in vitro that one of the domains responsible for directly binding to the YxxM motif, the N-terminal SH2 domain of p85 PI3K, has a sequence preference for peptides containing YMPM over other YxxM motifs³⁰. Of the six sites in the HER3 tail, only Y1054 has the sequence YMPM, while the others differ slightly, indicating that the superior ability of Y1054 to activate PI3K may be at least partially due to this greater binding affinity. Additionally, it's possible that due to either the differences in sequence or proximity to the kinase domain, that these sites may be differentially phosphorylated by their target kinase. The stoichiometry of individual site phosphorylation remains undetermined and could potentially vary depending on whether EGFR, HER2, or HER4 were playing the role of partner kinase, the concentration and duration of ligand stimulation, which of the two ligands is bound, and the activity of phosphatases toward each site.

Mass spectrometric analysis of tyrosines on EGFR has shown that phosphorylation of these sites is temporally regulated where Shc/Grb2 sites in the tail reach peak phosphorylation at four minutes post stimulation, while phosphorylation of Y998 which binds STAT5, PTP-2c, Shc, Crk, and Src increases through fifteen minutes³¹. Although such studies on HER3 are lacking, one can imagine that with thirteen potential substrate tyrosines (as well as multiple possible serine/threonine phosphorylation sites), phosphorylation of HER3 is also likely very dynamic and that this could dictate the activation of PI3K from individual YxxM sites. Determining the dynamics of context-dependent levels of tyrosine phosphorylation within the HER3 tail is an interesting question warranting further investigation.

Shc is a signaling scaffold protein that is activated through multiple tyrosine phosphorylation sites which serve as binding sites for downstream signaling molecules^{32, 33}. Shc

primarily signals to the Ras/MAPK pathway through recruitment of the Grb2/SOS complex^{34, 35}, however there is some evidence linking Shc to the activation of PI3K signaling. Cytokine receptors lacking direct PI3K binding sites can activate PI3K signaling through direct recruitment of Shc which then can scaffold a Grb2, Gab2, and PI3K signaling complex²⁵. Similarly, signaling generated from oscillatory shear stress in MG63 cells stimulated increased association of Shc to the p85 regulatory subunit of PI3K and enhanced PI3K signaling²⁶. Expression of a dominant-negative Gab2 mutant was able to block IL-3-induced PI3K-dependent proliferation in these cells providing further evidence of a Shc, Grb2, Gab2, PI3K signaling complex²⁶. In HER3 signaling, Shc has been shown to perform its canonical role of mediating activation of MAPK signaling. Mutation of the NPDY consensus binding motif for Shc disconnects HER3 from being able to activate the MAPK pathway²⁴. Our study demonstrates a new role for Shc in HER3 signaling in activation of the PI3K pathway. It is unclear what contribution this has in the context of normal physiological HER3 signaling to PI3K as Shc likely makes a minor contribution to the overall activation of PI3K signaling. However, it is possible that in cases of hypo-phosphorylation of the HER3 tail, simulated by our Y6F mutant, that the ability of Shc to activate both the PI3K and MAPK pathways may provide an advantage to cells. This effect could become more biologically significant in cancers where expression of Shc is upregulated. Additionally, a recent study reported a novel mechanism of redundancy in activation of PI3K in HER2-amplified cancers in which they found a weak direct binding site for PI3K in the intracellular tail of HER2³⁶. This demonstrates that in the context of high HER2 overexpression, PI3K activation from HER2 alone may be sufficient to drive cellular transformation and may not require HER3. These multiple mechanisms of redundancy in PI3K

activation in HER2/HER3 signaling illustrate how powerful and essential PI3K signaling is from this heterodimer pair.

2.5 MATERIALS AND METHODS

Cell Culture

Ba/F3 and plat-E cells were obtained from the Wells laboratory at UCSF. Ba/F3 cells were cultured in RPMI supplemented with 10% FBS, streptomycin/penicillin, HEPES, L-Glutamine, sodium pyruvate, and murine IL-3. Ba/F3 inhibitor assays were treated for a timecourse of 72 hours in supplemented media lacking IL-3 and additionally supplemented with 25ng/mL human NRG and containing PIK90, GDC0941, PD98059, TGX-221, or BH9 (Selleckchem). Plat-E cells were cultured in DMEM supplemented with 10% FBS, streptomycin/penicillin, puromycin, and blasticidin.

Creation of stable cell lines

HER3-mCherry constructs were cloned into the pMSCVhygro backbone and HER2- Δ tail-GFP was cloned into the pMSCVpuro backbone. Plat-E cells were transfected using FuGene6 (Promega) and cultured for 48 hours to generate virus. The supernatant was then collected, filtered, and used to resuspend 1×10^6 Ba/F3 cells. Cells were incubated with viral supernatant, IL-3, and what's called spinning at 1500rpm for 1.5 hours in a 6-well plate at room temperature. Fully supplemented Ba/F3 media was then added and cells were incubated for a further six hours at 37C before transferring to 10cm plates. After 24hours, cells were treated with appropriate selection antibiotic (puromycin or hygromycin) for 48 hours before sorting for GFP/mCherry-positive populations. Stable expression was maintained through culturing in media containing antibiotic.

Western blotting

Cells were lysed in RIPA buffer (50mM Tris pH 7.5, 150mM NaCl, 1mM EDTA, 1mM Na₃VO₄, 1mM NaF, 0.1% SDS, 0.1% deoxycholate, 1% IGEPAL CA-630) with protease inhibitor cocktail (Roche). Lysates were run on 10% SDS-PAGE and transferred (semi-dry) to PVDF membrane (EMD Millipore). Proteins were detected using: anti-HER3 (D22C5 XP – Cell Signaling), anti-HER3 (1B2E – Cell Signaling), anti-HER2 (D8F12 – Cell Signaling), anti-Akt, anti-pAkt pS473, anti-p44/42 MAPK (Erk1/2) (L34F12 – Cell Signaling), anti-Phospho-p44/42 MAPK (Erk1/2) (Thr202/Tyr204) (D13.14.4E, XP – Cell Signaling), anti-p85, anti-p110alpha, anti-p110beta, anti-p110delta, and anti-Shc (abcam). Secondary antibodies were anti-rabbit-IgG HRP-linked antibody (Cell Signaling), or anti-mouse IgG HRP-linked whole antibody (GE Healthcare Biosciences). Blots were developed using ECL/ECL Prime (Thermo Fisher Scientific).

Immunoprecipitation

HER3 or Shc antibody was conjugated to Protein A-sepharose beads (Life Technologies) using DMP crosslinker. Cells were lysed in RIPA buffer, cleared by centrifugation, and incubated with antibody-conjugated beads for 12-16 hours overnight at 4C. Beads were then washed and eluted using 3x SDS sample loading buffer and boiling at 90C for 10 minutes. Immunoprecipitates were analyzed by western blotting.

Viability assays

Ba/F3 cells were counted and the volume for 4×10^5 cells was pelleted and resuspended in 4mL normal Ba/F3 medium lacking IL-3 and supplemented with 25ng/mL NRG. Cells were cultured

for 72 hours. At 24, 48, and 72 hours, 1mL of cells was removed for assessment and 1mL fresh media was added back to plate. Viability was assayed by mixing 1 μ L Sytox Blue Dead Cell Stain into 1mL of cells, incubating for 8-10 minutes, and analyzing by flow cytometry on a BD FACS Aria III. Data analysis was done using FlowJo and plotted using GraphPad Prism or Excel.

2.6 REFERENCES

- 1 Cohen S, Fava RA, Sawyer ST. Purification and characterization of epidermal growth factor receptor/protein kinase from normal mouse liver. *Proc Natl Acad Sci U S A* 1982; 79: 6237-6241.
- 2 Schechter AL, Stern DF, Vaidyanathan L, Decker SJ, Drebin JA, Greene MI *et al.* The neu oncogene: an erb-B-related gene encoding a 185,000-Mr tumour antigen. *Nature* 1984; 312: 513-516.
- 3 Bargmann CI, Hung MC, Weinberg RA. The neu oncogene encodes an epidermal growth factor receptor-related protein. *Nature* 1986; 319: 226-230.
- 4 Kraus MH, Issing W, Miki T, Popescu NC, Aaronson SA. Isolation and characterization of ERBB3, a third member of the ERBB/epidermal growth factor receptor family: evidence for overexpression in a subset of human mammary tumors. *Proc Natl Acad Sci U S A* 1989; 86: 9193-9197.
- 5 Plowman GD, Whitney GS, Neubauer MG, Green JM, McDonald VL, Todaro GJ *et al.* Molecular cloning and expression of an additional epidermal growth factor receptor-related gene. *Proc Natl Acad Sci U S A* 1990; 87: 4905-4909.

- 6 Carraway KL, 3rd, Cantley LC. A new acquaintance for erbB3 and erbB4: a role for receptor heterodimerization in growth signaling. *Cell* 1994; 78: 5-8.
- 7 Guy PM, Platko JV, Cantley LC, Cerione RA, Carraway KL, 3rd. Insect cell-expressed p180erbB3 possesses an impaired tyrosine kinase activity. *Proc Natl Acad Sci U S A* 1994; 91: 8132-8136.
- 8 Soltoff SP, Carraway KL, 3rd, Prigent SA, Gullick WG, Cantley LC. ErbB3 is involved in activation of phosphatidylinositol 3-kinase by epidermal growth factor. *Mol Cell Biol* 1994; 14: 3550-3558.
- 9 Kim HH, Sierke SL, Koland JG. Epidermal growth factor-dependent association of phosphatidylinositol 3-kinase with the erbB3 gene product. *J Biol Chem* 1994; 269: 24747-24755.
- 10 Waterman H, Alroy I, Strano S, Seger R, Yarden Y. The C-terminus of the kinase-defective neuregulin receptor ErbB-3 confers mitogenic superiority and dictates endocytic routing. *EMBO J* 1999; 18: 3348-3358.
- 11 Thorpe LM, Yuzugullu H, Zhao JJ. PI3K in cancer: divergent roles of isoforms, modes of activation and therapeutic targeting. *Nat Rev Cancer* 2015; 15: 7-24.

- 12 McGlade CJ, Ellis C, Reedijk M, Anderson D, Mbamalu G, Reith AD *et al.* SH2 domains of the p85 alpha subunit of phosphatidylinositol 3-kinase regulate binding to growth factor receptors. *Mol Cell Biol* 1992; 12: 991-997.
- 13 Klippel A, Escobedo JA, Fantl WJ, Williams LT. The C-terminal SH2 domain of p85 accounts for the high affinity and specificity of the binding of phosphatidylinositol 3-kinase to phosphorylated platelet-derived growth factor beta receptor. *Mol Cell Biol* 1992; 12: 1451-1459.
- 14 Carpenter CL, Auger KR, Chanudhuri M, Yoakim M, Schaffhausen B, Shoelson S *et al.* Phosphoinositide 3-kinase is activated by phosphopeptides that bind to the SH2 domains of the 85-kDa subunit. *J Biol Chem* 1993; 268: 9478-9483.
- 15 Kaplan DR, Whitman M, Schaffhausen B, Pallas DC, White M, Cantley L *et al.* Common elements in growth factor stimulation and oncogenic transformation: 85 kd phosphoprotein and phosphatidylinositol kinase activity. *Cell* 1987; 50: 1021-1029.
- 16 Courtneidge SA, Heber A. An 81 kd protein complexed with middle T antigen and pp60c-src: a possible phosphatidylinositol kinase. *Cell* 1987; 50: 1031-1037.

- 17 Delcommenne M, Tan C, Gray V, Rue L, Woodgett J, Dedhar S. Phosphoinositide-3-OH kinase-dependent regulation of glycogen synthase kinase 3 and protein kinase B/AKT by the integrin-linked kinase. *Proc Natl Acad Sci U S A* 1998; 95: 11211-11216.
- 18 Persad S, Attwell S, Gray V, Mawji N, Deng JT, Leung D *et al.* Regulation of protein kinase B/Akt-serine 473 phosphorylation by integrin-linked kinase: critical roles for kinase activity and amino acids arginine 211 and serine 343. *J Biol Chem* 2001; 276: 27462-27469.
- 19 Fruman DA, Chiu H, Hopkins BD, Bagrodia S, Cantley LC, Abraham RT. The PI3K Pathway in Human Disease. *Cell* 2017; 170: 605-635.
- 20 Shoelson SE, Chatterjee S, Chaudhuri M, White MF. YMXM motifs of IRS-1 define substrate specificity of the insulin receptor kinase. *Proc Natl Acad Sci U S A* 1992; 89: 2027-2031.
- 21 Hellyer NJ, Kim MS, Koland JG. Heregulin-dependent activation of phosphoinositide 3-kinase and Akt via the ErbB2/ErbB3 co-receptor. *J Biol Chem* 2001; 276: 42153-42161.
- 22 Daley GQ, Baltimore D. Transformation of an interleukin 3-dependent hematopoietic cell line by the chronic myelogenous leukemia-specific P210bcr/abl protein. *Proc Natl Acad Sci U S A* 1988; 85: 9312-9316.

- 23 Riese DJ, Kim ED, Elenius K, Buckley S, Klagsbrun M, Plowman GD *et al.* The epidermal growth factor receptor couples transforming growth factor-alpha, heparin-binding epidermal growth factor-like factor, and amphiregulin to Neu, ErbB-3, and ErbB-4. *J Biol Chem* 1996; 271: 20047-20052.
- 24 Vijapurkar U, Cheng K, Koland JG. Mutation of a Shc binding site tyrosine residue in ErbB3/HER3 blocks heregulin-dependent activation of mitogen-activated protein kinase. *J Biol Chem* 1998; 273: 20996-21002.
- 25 Gu H, Maeda H, Moon JJ, Lord JD, Yoakim M, Nelson BH *et al.* New role for Shc in activation of the phosphatidylinositol 3-kinase/Akt pathway. *Mol Cell Biol* 2000; 20: 7109-7120.
- 26 Lee DY, Li YS, Chang SF, Zhou J, Ho HM, Chiu JJ *et al.* Oscillatory flow-induced proliferation of osteoblast-like cells is mediated by alphavbeta3 and beta1 integrins through synergistic interactions of focal adhesion kinase and Shc with phosphatidylinositol 3-kinase and the Akt/mTOR/p70S6K pathway. *J Biol Chem* 2010; 285: 30-42.

- 27 Knight ZA, Gonzalez B, Feldman ME, Zunder ER, Goldenberg DD, Williams O *et al.* A pharmacological map of the PI3-K family defines a role for p110alpha in insulin signaling. *Cell* 2006; 125: 733-747.
- 28 Fedi P, Pierce JH, di Fiore PP, Kraus MH. Efficient coupling with phosphatidylinositol 3-kinase, but not phospholipase C gamma or GTPase-activating protein, distinguishes ErbB-3 signaling from that of other ErbB/EGFR family members. *Mol Cell Biol* 1994; 14: 492-500.
- 29 Hellyer NJ, Cheng K, Koland JG. ErbB3 (HER3) interaction with the p85 regulatory subunit of phosphoinositide 3-kinase. *Biochem J* 1998; 333 (Pt 3): 757-763.
- 30 Songyang Z, Shoelson SE, Chaudhuri M, Gish G, Pawson T, Haser WG *et al.* SH2 domains recognize specific phosphopeptide sequences. *Cell* 1993; 72: 767-778.
- 31 Schulze WX, Deng L, Mann M. Phosphotyrosine interactome of the ErbB-receptor kinase family. *Mol Syst Biol* 2005; 1: 2005 0008.
- 32 van der Geer P, Wiley S, Gish GD, Pawson T. The Shc adaptor protein is highly phosphorylated at conserved, twin tyrosine residues (Y239/240) that mediate protein-protein interactions. *Curr Biol* 1996; 6: 1435-1444.

- 33 Lennartsson J, Blume-Jensen P, Hermanson M, Ponten E, Carlberg M, Ronnstrand L. Phosphorylation of Shc by Src family kinases is necessary for stem cell factor receptor/c-kit mediated activation of the Ras/MAP kinase pathway and c-fos induction. *Oncogene* 1999; 18: 5546-5553.
- 34 Pelicci G, Lanfrancone L, Grignani F, McGlade J, Cavallo F, Forni G *et al.* A novel transforming protein (SHC) with an SH2 domain is implicated in mitogenic signal transduction. *Cell* 1992; 70: 93-104.
- 35 Rozakis-Adcock M, McGlade J, Mbamalu G, Pelicci G, Daly R, Li W *et al.* Association of the Shc and Grb2/Sem5 SH2-containing proteins is implicated in activation of the Ras pathway by tyrosine kinases. *Nature* 1992; 360: 689-692.
- 36 Ruiz-Saenz A, Dreyer C, Campbell MR, Steri V, Gulizia NP, Moasser MM. HER2 amplification in tumors activates PI3K/Akt signaling independent of HER3. *Cancer Res* 2018.

2.7 FIGURES

Figure 1.

HER3 is unusual among PI3K binding proteins in having six YxxM sites **(A)** Chart analyzing the number of YxxM sites in each of 86 PI3K binding proteins.

Figure 2.

All six YxxM motifs in HER3 contribute to PI3K signaling **(A)** Parental Ba/F3 cells, or Ba/F3 cells expressing HER2- Δ tail-GFP or HER3-mCherry alone or in combination were cultured in growth media lacking IL-3 and supplemented with 25ng/mL NRG for 72 hours. Cell viability was assessed every 24 hours. **(B)** **(C)** Comparison of viability between parental Ba/F3 cells to HER2- Δ tail-GFP + HER3-mCherry-expressing Ba/F3 cells treated pan PI3K inhibitor +/- 10uM GDC0941 **(B)** or 5 μ M PIK90 **(C)** for 48 hours. **(D)** Schematic representing three sets of HER3 mutant constructs designed to probe single YxxM site function. **(E)** Ba/F3 cells co-expressing HER2- Δ tail-GFP with single site knock-IN HER3-mCherry variants were cultured in growth media lacking IL-3 and supplemented with 25ng/mL for 72 hours. Cell viability was assessed every 24 hours. **(F)** Ba/F3 cells co-expressing HER2- Δ tail-GFP with single site knock-OUT HER3-mCherry variants were cultured in growth media lacking IL-3 and supplemented with 25ng/mL for 72 hours. Cell viability was assessed every 24 hours.

Figure 3.

Even in the absence of all YxxM sites, HER3 can maintain Ba/F3 viability. **(A)** Ba/F3 cells co-expressing HER2- Δ tail-GFP with either wildtype or HER3-Y6F HER3-mCherry variants were

cultured in growth media lacking IL-3 and supplemented with 25ng/mL for 72 hours. Cell viability was assessed every 24 hours. **(B)** Parental Ba/F3, and Ba/F3 cells stably expressing HER2- Δ tail-GFP with either wildtype or HER3-Y6F HER3-mCherry were cultured in growth media lacking IL-3, supplemented with 25ng/mL, and in the presence of a pan-PI3K inhibitor (5 μ M PIK90), a MEK inhibitor (10 μ M PD98059), or both for 72 hours. Data presented is taken from the 48 hour time-point averaged over three independent biological replicates \pm SEM. **(C)** Ba/F3 cells stably expressing HER2- Δ tail-GFP with either wildtype or HER3-Y6F HER3-mCherry were immunoprecipitated with anti-HER3-conjugated Protein A beads and assayed for the presence of PI3K by western blot. Lysates were assayed for total HER2 and HER3 protein levels and activation of Akt by western blot. **(D)** Ba/F3 cells stably expressing HER2- Δ tail-GFP with either wildtype or HER3-Y6F HER3-mCherry were counted and cultured in growth media lacking IL-3 and supplemented with 25ng/mL NRG for 5 minutes, or 24, 48, or 72 hours. Lysates were assayed for activation of Akt and Erk.

Figure 4

Recruitment of Shc to HER3 activates PI3K in the absence of YxxM motifs. **(A)** Schematic of HER3-mCherry tail deletion constructs. Ba/F3 cells stably expressing HER2- Δ tail-GFP with HER3-mCherry deletion constructs were counted and cultured in growth media lacking IL-3, and supplemented with 25ng/mL NRG for 72 hours. Viability was assessed every 24 hours. **(B)** Ba/F3 cells stably expressing HER2- Δ tail-GFP with either wildtype or Y6F, Y1328F, or Y6F-Y1328F variants of HER3-mCherry were immunoprecipitated with anti-HER3-conjugated Protein A beads and assayed for the presence of Shc by western blot. **(C)** Ba/F3 cells stably expressing HER2- Δ tail-GFP with either wildtype or Y6F, Y1328F, or Y6F-Y1328F variants of

HER3-mCherry were counted and cultured in growth media lacking IL-3, and supplemented with 25ng/mL NRG for 72 hours. Viability was assessed every 24 hours. **(D)** HEK293 cells transiently co-expressing HER2- Δ tail-GFP with either wildtype or Y6F, or Y6F-Y1328F variants of HER3 were serum starved for six hours and stimulated with 25ng/mL NRG for 5 minutes. Lysates were assayed for activation of Akt by western blot.

Figure 5

The Y1054 and Y1289 YxxM sites are stronger potentiators of cell survival than the other HER3 YxxM sites. **(A)** Schematic of Shc site mutation (Y1328F) combined with HER3-mCherry single-site knock-IN constructs. **(B)** Ba/F3 cells co-expressing HER2- Δ tail-GFP with single site knock-IN+Y1328F HER3-mCherry variants were cultured in growth media lacking IL-3 and supplemented with 25ng/mL for 72 hours. Cell viability was assessed every 24 hours. **(C)** Quantification of 72h timepoint shown in panel B for ease of comparison between knock-IN mutants.

Figure 6

HER3 signals through both the p110 α and p110 β isoforms of PI3K **(A)** Ba/F3 cells stably expressing HER2- Δ tail-GFP with wildtype HER3-mCherry were cultured in growth media lacking IL-3 and supplemented with 25ng/mL in the presence of p110 α specific inhibitor (20 μ M BH9) or p110 β inhibitor (20 μ M TGX-221) for 72 hours. Cell viability was assessed every 24 hours. **(B)** Ba/F3 cells co-expressing HER2- Δ tail-GFP with single site knock-IN+Y1328F HER3-mCherry variants were cultured in growth media lacking IL-3 and supplemented with

25ng/mL in the presence of p110 α specific inhibitor (10 μ M BH9) or p110 β inhibitor (10 μ M TGX-221) for 72 hours. Cell viability was assessed every 24 hours

Figure 7

Evolutionary analysis of YxxM motifs in HER3 suggests Y1054 may be the most conserved in the HER3 tail. **(A)** Analysis of one hundred HER3 orthologues for the number of YxxM motifs in the C-terminal tail. **(B)** Sequence logos for the C-terminal tails of mammalian and non-mammalian vertebrate HER3 orthologues. **(C)** Amino acid sequences of the six YxxM sites in the C-terminal tail of HER3.

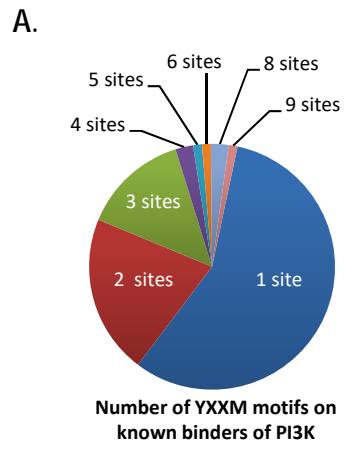


Figure 1. HER3 is unusual among PI3K binding proteins in having six YxxM sites

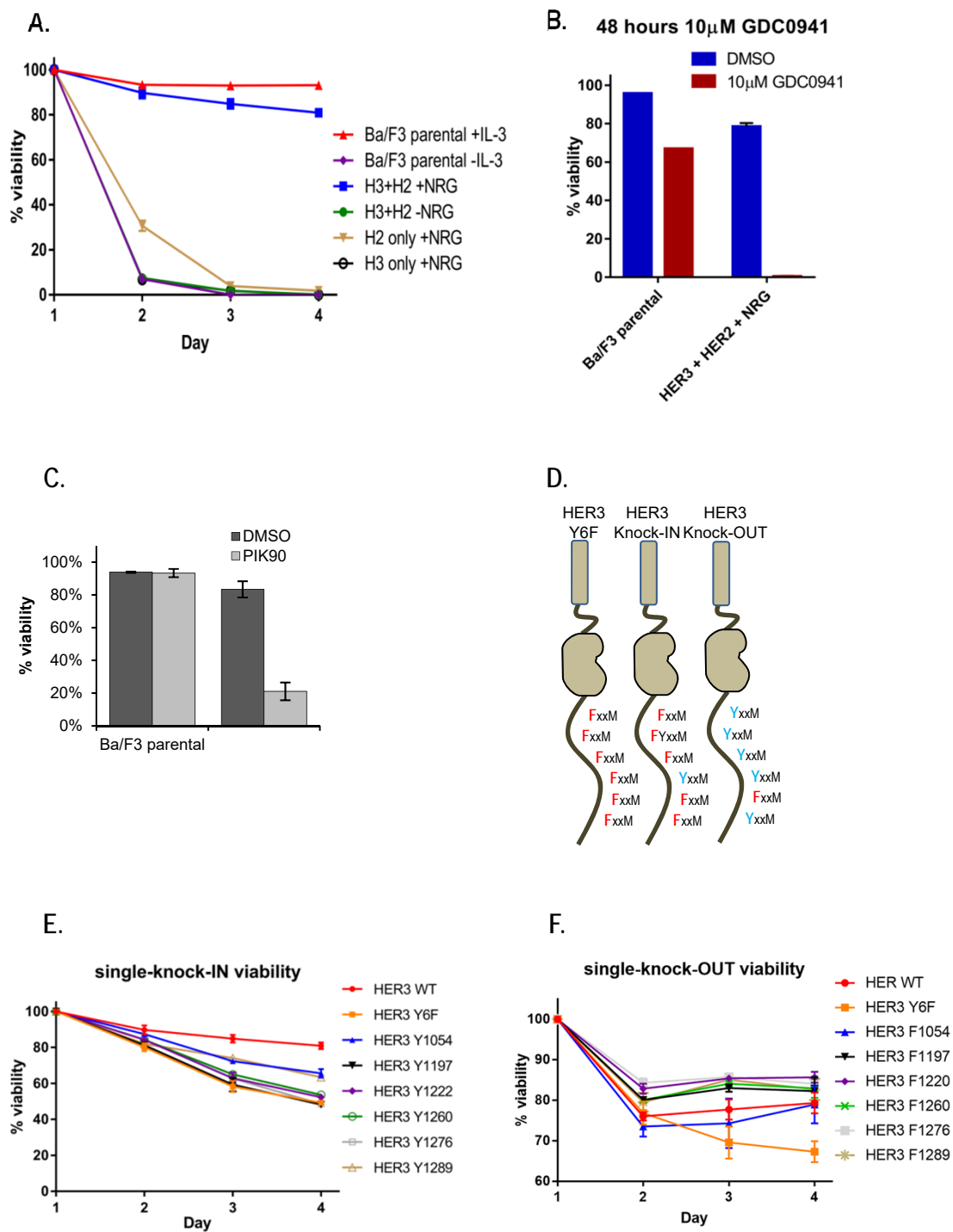


Figure 2. All six YxxM motifs in HER3 contribute to PI3K signaling

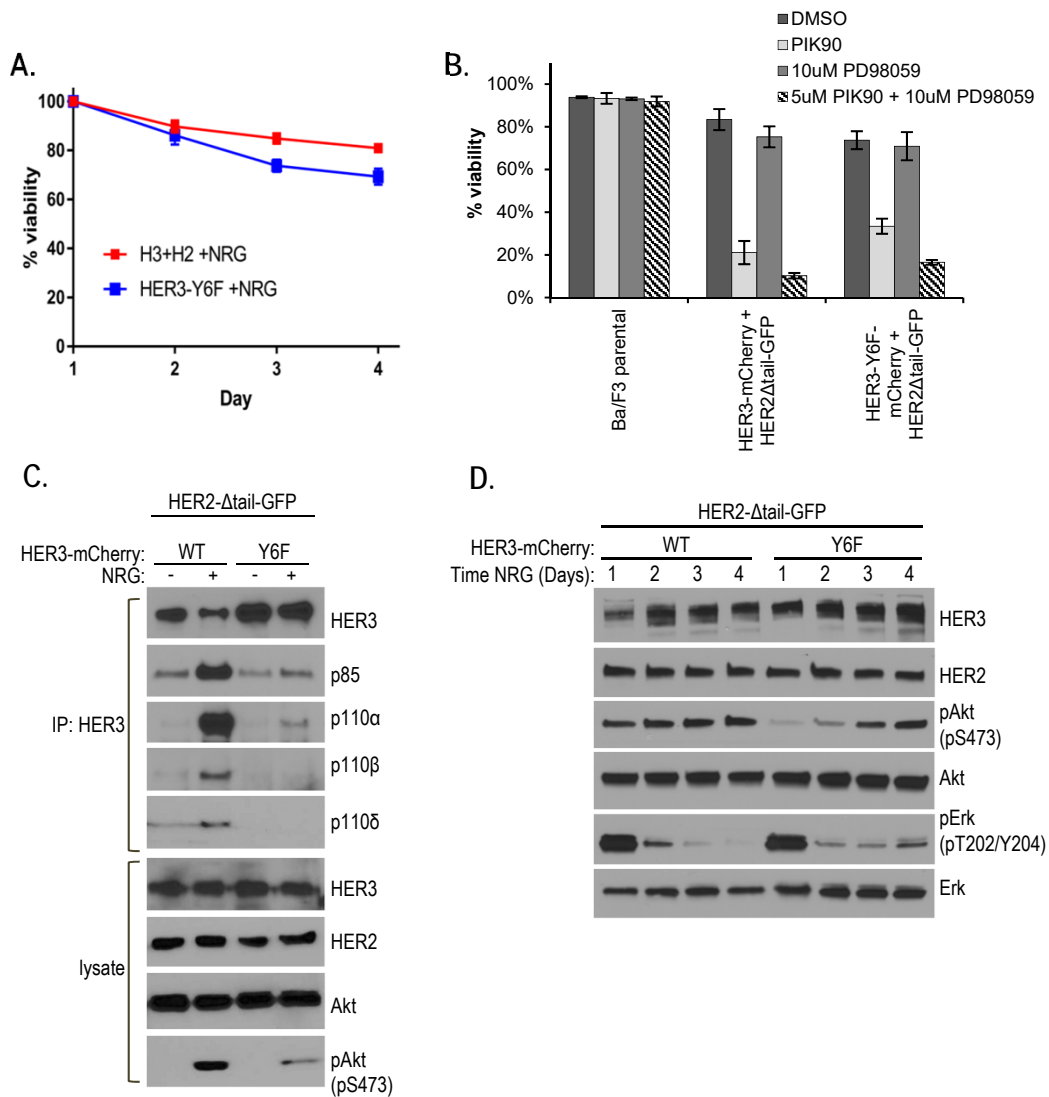


Figure 3 Even in the absence of all YxxM sites, HER3 can maintain Ba/F3 cell viability

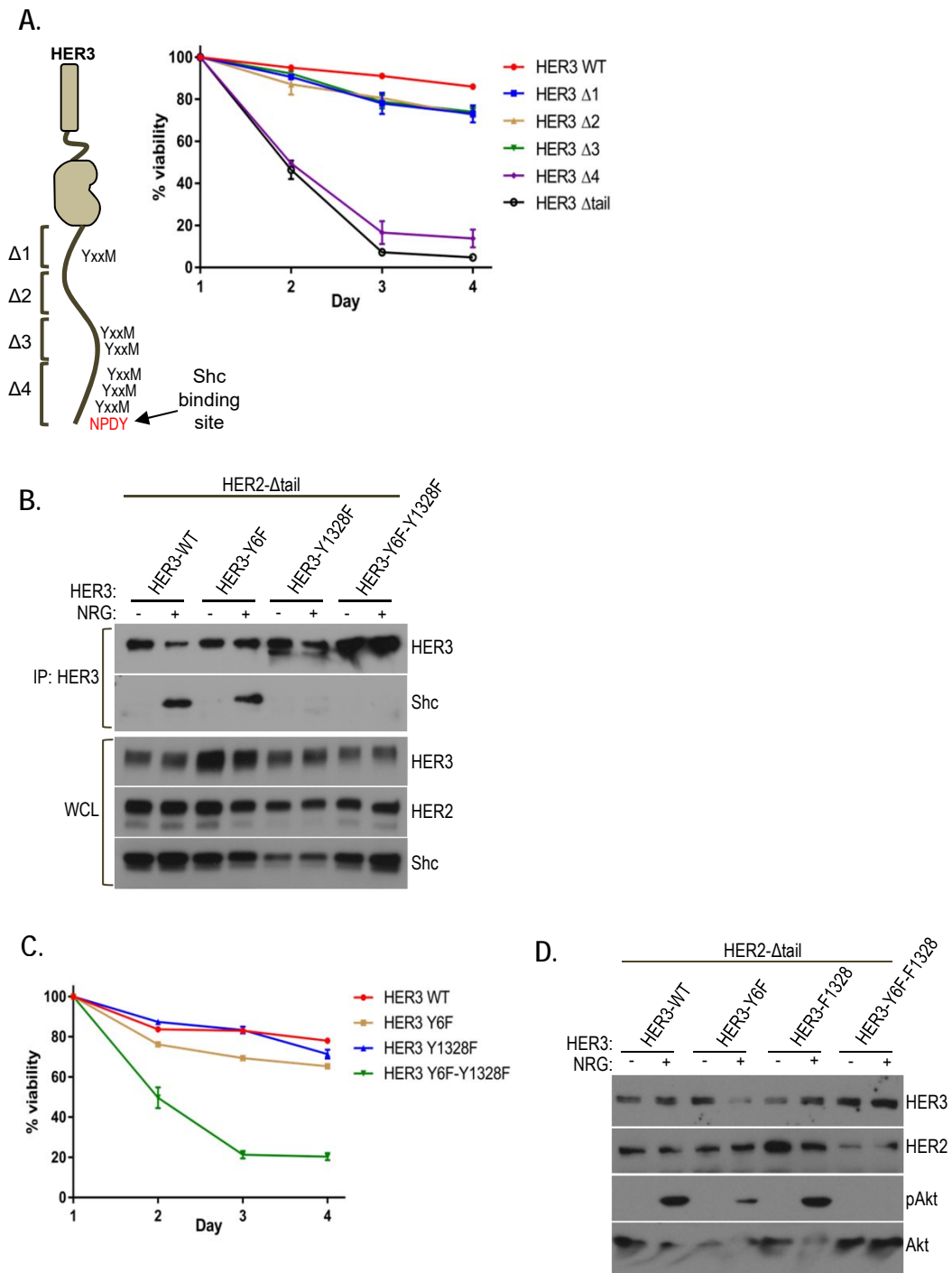


Figure 4 Recruitment of SHC to HER3 activates PI3K in the absence of YxxM motifs

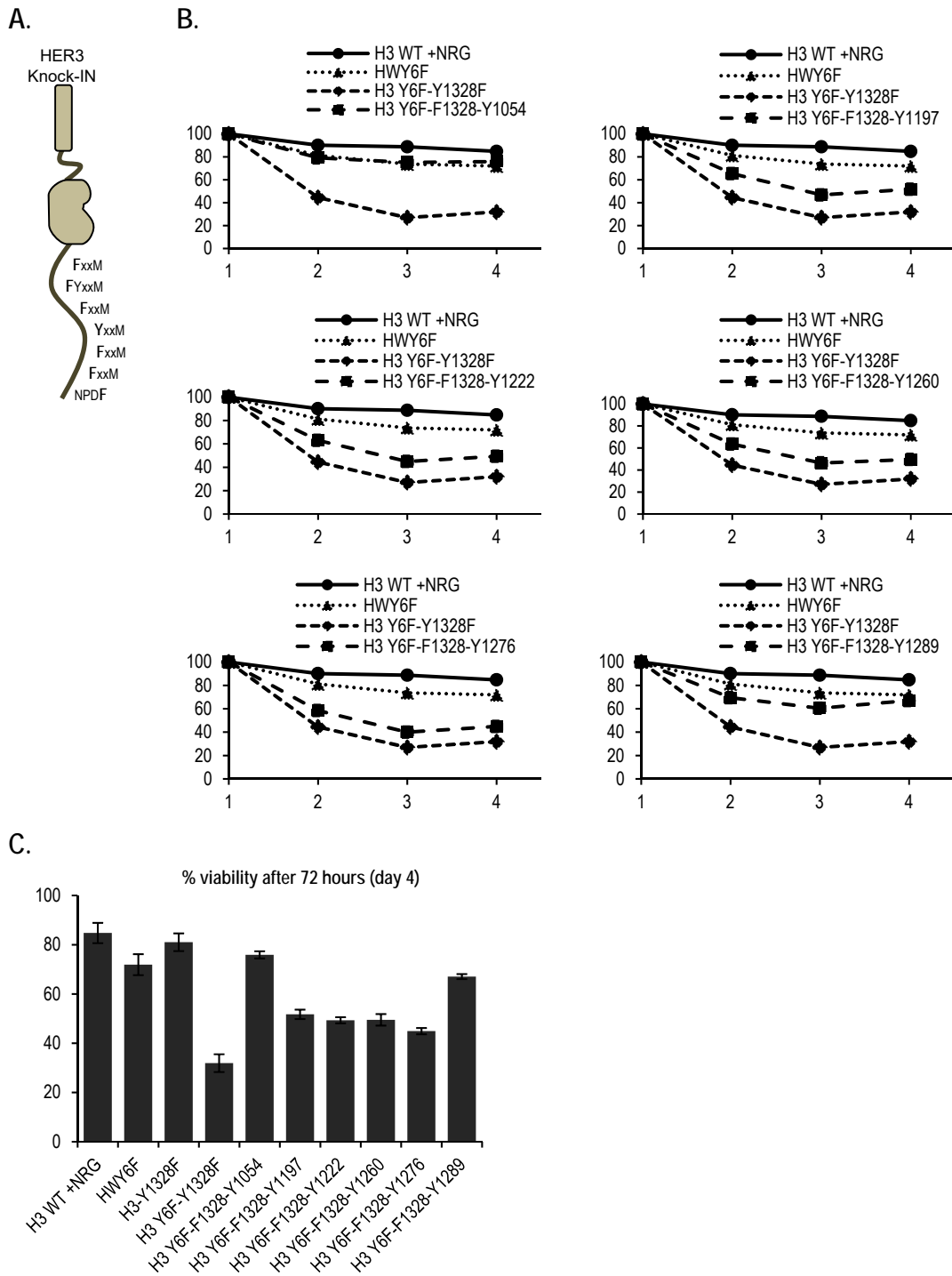
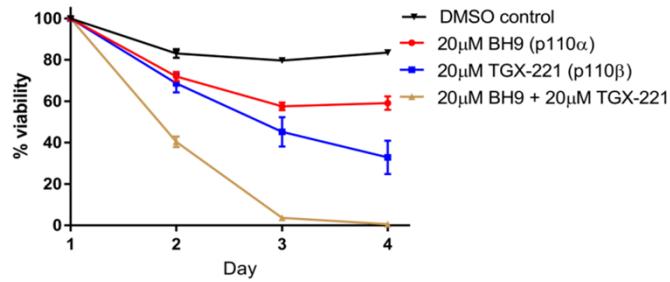


Figure 5 The Y1054 YxxM site is a stronger potentiator of cell survival than the other HER3 YxxM sites

A.

WT-HER3 with isoform-specific p110 inhibitors



B.

**Shc + YxxM mutants
Isoform specific inhibitor viability (48 hours)**

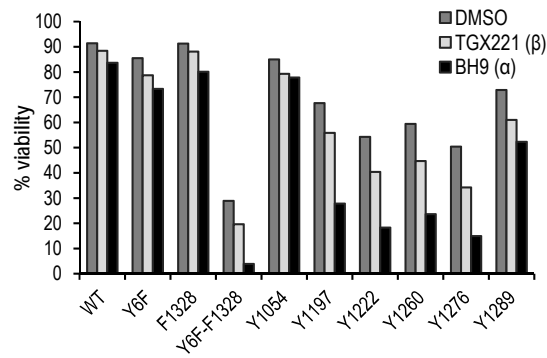
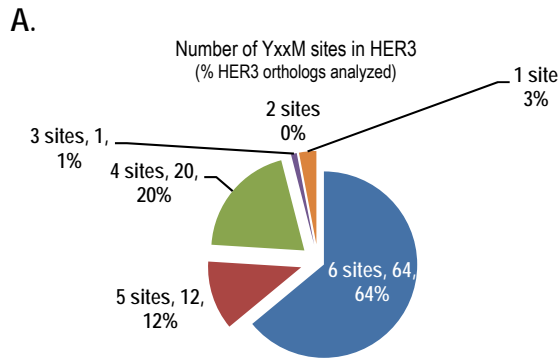
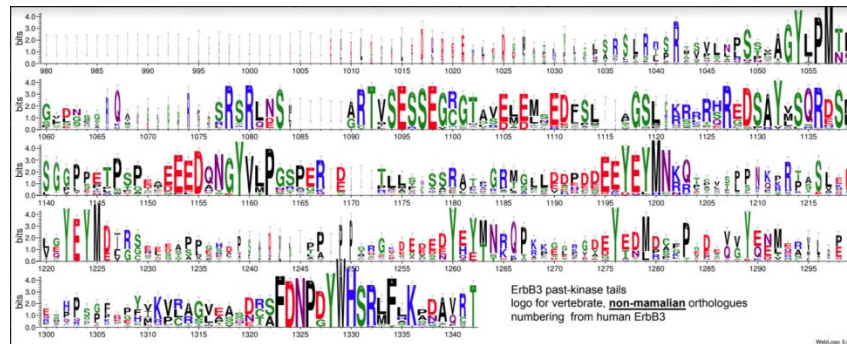


Figure 6 HER3 signals through both p110 α and p110 β isoforms of PI3K



B.



C.

Tyrosine in HER3 tail	YxxM motif
Y1054	YMPM
Y1197	YEYM
Y1222	YEYM
Y1260	YEYM
Y1276	YAAM
Y1289	YEEM

Figure 7. Evolutionary analysis of YxxM motifs in HER3 suggests Y1054 may be the most conserved

Publishing Agreement

It is the policy of the University to encourage the distribution of all theses, dissertations, and manuscripts. Copies of all UCSF theses, dissertations, and manuscripts will be routed to the library via the Graduate Division. The library will make all theses, dissertations, and manuscripts accessible to the public and will preserve these to the best of their abilities, in perpetuity.

I hereby grant permission to the Graduate Division of the University of California, San Francisco to release copies of my thesis, dissertation, or manuscript to the Campus Library to provide access and preservation, in whole or in part, in perpetuity.

Author Signature *Nicol Michael Frajer* Date 06/08/2018